NASA

Technical Memorandum 85061

(NASA-TM-85061) ASSESSMENT OF FLYWHEEL ENERGY STORAGE FOR SPACECRAFT POWER SYSTEMS (NASA) 53 p HC A04/MF A01 CSCL 22B

N83-33941

Unclas
G3/20 36153

ASSESSMENT OF FLYWHEEL ENERGY STORAGE FOR SPACECRAFT POWER SYSTEMS

G. E. Rodriguez
P. A. Studer
D. A. Baer

MAY 1983

National Aeronautics and
Space Administration

Goddard Space Flight Center
Greenbelt, Maryland 20771

TM-85061

ASSESSMENT OF FLYWHEEL ENERGY STORAGE

FOR

SPACECRAFT POWER SYSTEMS

G. Ernest Rodriguez
Philip A. Studer
David A. Baer

May 1983

GODDARD SPACE FLIGHT CENTER
Greenbelt, Maryland

All measurement values are expressed in the International System of Units (SI) in accordance with NASA Policy Directive 2220.4, paragraph 4.

ABSTRACT

The feasibility of inertial energy storage in a spacecraft power system is evaluated on the basis of a conceptual integrated design that encompasses a composite rotor, magnetic suspension, and a permanent magnet (PM) motor/generator for a 3-kW orbital average payload at a bus distribution voltage of 250 volts dc. The conceptual design, which evolved at the Goddard Space Flight Center (GSFC), is referred to as a "Mechanical Capacitor." The baseline power system configuration selected is a series system employing peak-power-tracking for a Low Earth-Orbiting application. Power processing, required in the motor/generator, provides a potential alternative that can only be achieved in systems with electrochemical energy storage by the addition of power processing components. One such alternative configuration provides for peak-power-tracking of the solar array and still maintains a regulated bus, without the expense of additional power processing components. Precise speed control of the two counterrotating wheels is required to reduce interaction with the attitude control system (ACS) or alternatively, used to perform attitude control functions. Critical technologies identified are those pertaining to the energy storage element and are prioritized as composite wheel development, magnetic suspension, motor/generator, containment, and momentum control. Comparison with a 3-kW, 250-Vdc power system using either NiCd or NiH_2 for energy storage results in a system in which inertial energy storage offers potential advantages in lifetime, operating temperature, voltage regulation, energy density, charge control, and overall system weight reduction. The key disadvantages are attitude control interface and launch constraints.

CONTENTS

CONTENTS (Continued)

ILLUSTRATIONS

TABLES

EXECUTIVE SUMMARY

Energy storage and conversion have been and will continue to be key elements in developing earth applications and science-oriented spacecraft. Most spacecraft flown to date utilize photovoltaic technology for energy conversion and electrochemical technology for energy storage. Performance improvements of these technologies, as well as the search for new ones, are constantly pursued through various research and development programs. The development of composite materials and their application in super flywheels has aroused considerable interest in spacecraft power system applications because of the potential high energy density. Under the NASA Research and Technology Objective and Plan (RTOP) titled "Advanced Power System Technology" (RTOP 506-55-76), task 4 was initiated to develop concepts, perform feasibility analysis, design, develop, and demonstrate high overall system efficiency and reliability in a spacecraft power system with inertial energy storage. This study, which evolved from the development at GSFC of the "Mechanical Capacitor" (References 1 through 6), focused on Low Earth Orbit (LEO) missions. This mechanical capacitor is based on an integrated design incorporating the following three key technologies:

- Composite Materials
- Magnetic Suspension
- Permanent Magnet DC Motor/Generator

General guidelines, initial specific guidelines, efficiency train, and mass estimates for a spacecraft power system are documented in Reference 7 for this task. The power level under consideration was selected between the range of 2.5 to 25 kW, with a modular approach consisting of a basic 2.5-kW module. This power range fills the gap between presently applied technology and future large-scale systems now being studied.

The feasibility of inertial energy storage in a spacecraft power system with respect to power system configuration, power distribution, and spacecraft compatibility is not found to be dependent on the development of any technology other than the inertial energy storage element itself. The energy storage element under consideration (Figure 1) has potential advantages of long lifetime (20 to 30 years), high temperature (50°C) waste heat rejection, simple charge detection and control (wheel speed), inherent high voltage (>200 V) implementation (motor/generator design), high pulse power capability, higher energy density (Wh/kg) than NiCd, and higher volumetric density (Wh/m^3) than NiH_2. The relatively large momentum in inertial energy storage wheels must be precisely controlled to minimize attitude control disturbances or alternatively, used to perform the attitude control functions with potential overall system mass savings. In either case, a direct interface is required with the ACS.

Self-discharge, or energy storage efficiency, containment, and launch restrictions are three areas that require careful consideration in the intended application. For example, in LEO applications the self-discharge of the inertial energy storage element does not significantly affect the overall system performance. In unmanned vehicles, containment requirements would be less demanding than in

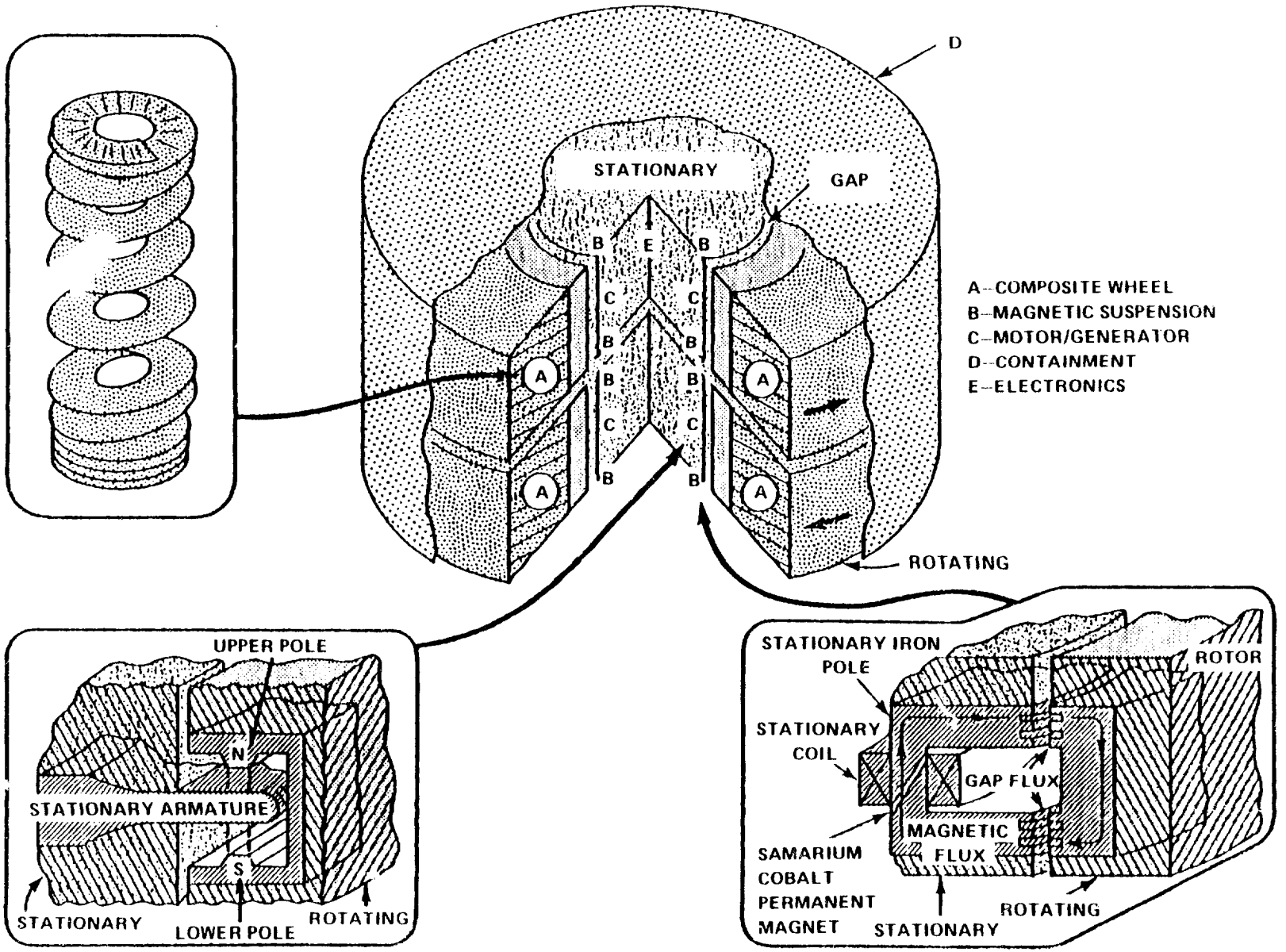

Figure 1. Spacecraft flywheel power system, conceptual flywheel design.

manned vehicles. Spacecraft acquisition during launch may require electrochemical energy storage in a launch mode in which the energy storage wheels must be "locked."

The potential advantages will only be realized by developing a complete integrated design that encompasses composite rotor technology (high energy density), magnetic suspension (high lifetime, low losses), permanent magnet (PM) ironless armature, brushless motor/generator technology (high efficiency of conversion and low standby power), and suitable containment of the wheel in the event of wheel or system failure. Although encouraging results have been obtained individually in these technologies, a high degree of risk is involved in obtaining a successful integrated design.

A considerable effort with an accompanying high level of funding is required for developing a spacecraft power system with inertial energy storage and its demonstration. However, since the energy storage element itself is found to be the only critical technology, the required level of funding can be postponed, the risk can be reduced by initially concentrating on the energy storage element, and pending successful demonstration of performance, a complete power system can then be pursued. This requires an extension of time of the original Program and Specific Objectives (PASO) target.

The hardware required to demonstrate the proof of principle of inertial energy storage for spacecraft power systems can be limited to essentially a single energy storage wheel with magnetic suspension, PM motor/generator, control electronics, and the necessary bench test equipment. Following successful completion, this hardware can then be expanded by the development of suitable containment and the addition of a second counterrotating wheel system to demonstrate momentum control. If this phase of development is found to be compatible with attitude control system requirements, the program should then proceed toward the development of a complete power system with attendant ground tests.

Critical technologies within the energy storage element are identified and prioritized as follows:

I. "Thick Rim" Wheel

II. Magnetic Suspension

III. Motor/Generator

IV. Containment

V. Momentum Control

The development of a suitable "thick rim" wheel is the key to the successful development of the inertial energy storage element for spacecraft power system applications. The development of the "thick rim" will provide the volumetric efficiency required. The development of the magnetic suspension, motor/generator, and containment systems depends heavily on the characteristics of the wheel. A wheel design with an ID/OD ratio of approximately 0.6 to 0.4 is required; typical wheels

presently developed exhibit an ID/OD ratio of 0.8 to 0.7. Two potential designs have evolved from the Department of Energy's (DOE's) flywheel development program: the AVCO woven spiral design and the General Electric (GE) hybrid rotor with the soft matrix. Both designs need further development. Recent termination of the DOE flywheel development program has curtailed further development of these two designs. A recent test (March 1983) completed at the Oak Ridge National Laboratory on the GE hybrid rotor design indicates encouraging results by demonstrating 10^4 cycles and an energy density capability of 66.8 Wh/kg (burst). These data support the assumptions used in the design calculations in this report (45 Wh/kg operational, 10^5 cycles) and increase the confidence that high performance composite rotors for spacecraft applications can be produced.

ASSESSMENT OF FLYWHEEL ENERGY STORAGE FOR SPACECRAFT POWER SYSTEMS

G. Ernest Rodriguez,
Philip A. Studer, and David A. Baer
NASA/Goddard Space Flight Center
Greenbelt, Maryland

INTRODUCTION

Energy storage and conversion have been and will continue to be key elements in developing earth applications and science-oriented spacecraft. Most spacecraft flown to date utilize photovoltaic technology for energy storage. Performance improvements of these technologies, as well as the search for new ones, are constantly pursued through various research and development programs. The development of composite materials and their application in super flywheels has aroused considerable interest in spacecraft power system applications because of the potential high energy density. Under the NASA Research and Technology Objective and Plan (RTOP) titled "Advanced Power System Technology" (RTOP 506-55-76), task 4 was initiated to develop concepts, perform feasibility analysis, design, develop, and demonstrate high overall system efficiency and reliability in a spacecraft power system with inertial energy storage. This study, which evolved from the development at GSFC of the "Mechanical Capacitor" (References 1 through 6), focused on Low Earth Orbit (LEO) missions. The mechanical capacitor is based on an integrated design incorporating the following three key technologies:

- Composite Materials
- Magnetic Suspension
- Permanent Magnet Motor/Generator

General guidelines, initial specific guidelines, efficiency train, and mass estimates for a spacecraft power system are documented in Reference 7 for this task. A baseline design of a power system for spacecraft using inertial energy storage is documented in Reference 8.

POWER SYSTEM DISCUSSION

Power Level

Spacecraft power requirements over the last decade have typically ranged from 200 watts to 2 kW, and future large-scale spacecraft power requirements have been projected to be in the range of 25 to 100 kW. This feasibility study concentrated within the power range of 2.5 to 25 kW, with

modularity in mind to allow growth in power with the basic building block of a 2.5-kW power subsystem module. Paralleling of modules minimizes the load interface during growth by allowing standardization of the bus voltage for a given power range. Typical power subsystems have been standardized using a direct current (dc) bus voltage of 28 volts, which represents a harness design of approximately 100 amperes. Selection of a bus voltage that is one order of magnitude higher would allow a similar harness design for the power range of interest. Thus, a nominal bus voltage of 250 volts was selected for the 2.5-kW module, and with ten modules in parallel, a power capability of 25 kW could be realized. The 250-volt bus would allow growth potential for power systems up to 100 kW as well. An example of future power systems operating at this level is the "Advanced Aircraft Electric Power System" development for future military and commercial aircraft using a dc power distribution system of 270 volts (References 9 through 11).

Power Distribution

Three-phase alternating current (ac), inherent in the mechanism of the motor/generator, does not offer a significant advantage for power distribution primarily because of power quality. Variable voltage (250 V ±20%) and low frequency (3 kHz ±20%) are characteristics of the baseline design. Additional power conditioning would be required to increase the frequency to a sufficiently high level (20 to 40 kHz); otherwise, the corresponding "magnetics" mass at the system level becomes prohibitive. In addition, frequency synchronization of a pair of wheels and of all modules in parallel becomes complex. Frequency synchronization within a pair of counterrotating wheels would inhibit speed control as a method of achieving net zero momentum disturbance. Based on these three factors—power quality, synchronization complexity, and momentum control, dc power distribution is selected as the most advantageous for the power system.

Power System Configuration

Most spacecraft power system configurations can be categorized into two basic types:

- Series system
- Shunt system

Series/shunt applies to the power processing element that is used to control the solar-array power. Although combinations or variations of these two are used for mission-unique applications, generally, the series system is used in LEO missions and the shunt system is used in GEO missions. The series element allows maximum extraction of solar-array power (peak-power-tracking) as the array temperature (and thus array power) undergoes large temperature excursions, typical of LEO, and provides a means for keeping the excess array power distributed on the array when not required by the spacecraft load. In GEO missions, the array temperature remains constant during the extended sunlight periods, and the shunt element provides an efficient means for transferring the array power to the spacecraft load by shunting only what is in excess.

Since electrical characteristics of the baseline inertial energy storage element are similar to those of an electrochemical element, the system configuration is governed by the mission more than by the

system elements. However, alternative power system configurations can be achieved with inertial energy storage that cannot be realized with electrochemical energy storage without the addition of external power conditioning components. For example, the direct energy transfer (DET) system, or shunt configuration (Figure 2a), can be achieved simply by pulsewidth modulation of the power switching components within the motor/generator to provide the charge/discharge regulator function, normally provided by the additional power conditioning components shown in Figure 2b for an electrochemical system. The shunt regulator function is still required in either case. The pulsewidth modulation of the power switching components does not significantly alter the net efficiency of the flywheel system. However, in the electrochemical system, a typical loss penalty of approximately 10 percent for the charge regulator and 10 percent for the discharge regulator is incurred, resulting in an overall loss of 20 percent.

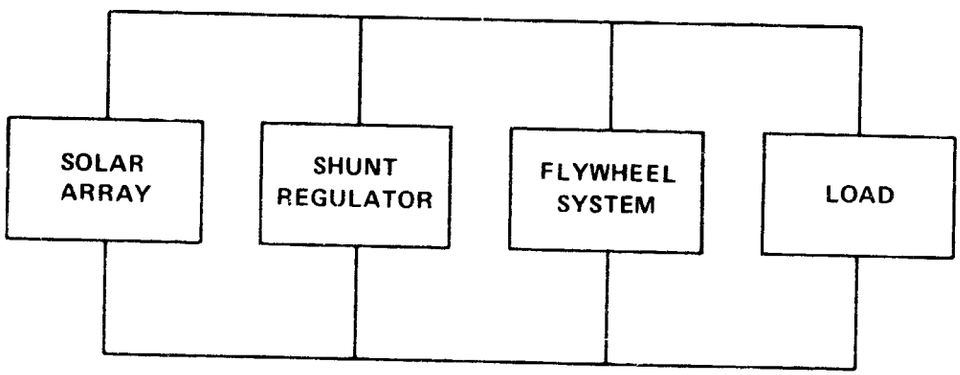

(a) Inertial Energy Storage

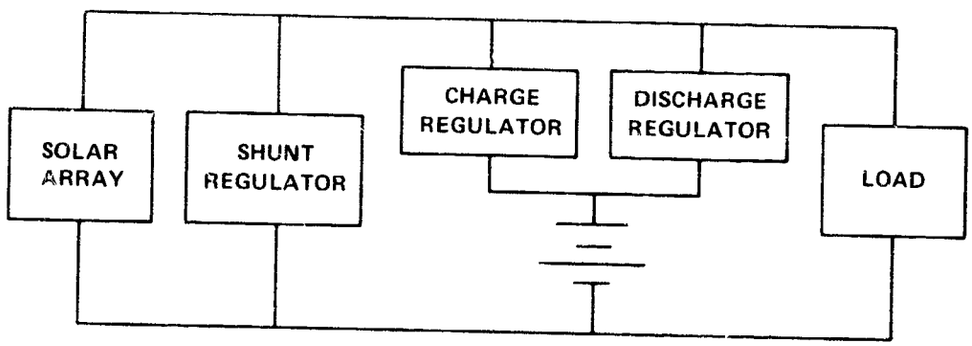

(b) Electrochemical Storage

Figure 2. Direct energy transfer (DET) system.

A departure from the baseline design is shown in Figure 3. This configuration provides the capability to peak-power-track the solar array by pulsewidth modulation of the power switching components of the motor. Similarly, by pulsewidth modulation of the power switching components within the generator, the load bus can be regulated. Separate motor/generator windings and additional switching transistors would be required for this variation, as described in further detail in the section on power conditioning. Although a mass savings is realized by eliminating the mass of the series element, a mass penalty is incurred in the flywheel system by the required additional motor winding and power switching components. However, the net result is that a potential mass savings is realized because the circuit elements and housing required by the series element are eliminated. An increase in thermal dissipation within the flywheel system would be expected since all the solar-array power must funnel through the motor. Further detailed tradeoff studies are necessary for evaluating this configuration.

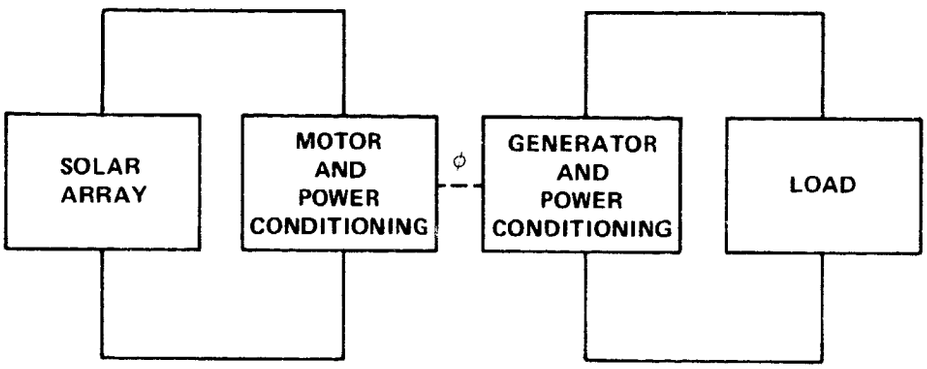

Figure 3. Peak-power-tracker, regulated bus system.

In GEO missions, the shunt system configuration requires a shunt regulator capable of dissipating almost all the solar-array power. This can cause a serious thermal design problem, particularly in the 2- to 25-kW power range. An alternative to the shunt dissipative regulator is the "switching" shunt regulator, which can be achieved by shunting sections of the array using diodes to isolate the array section from the bus and a switching transistor per array section to shunt it The switching transistors can be controlled by using sequential control for coarse control and limit cycle control for fine control. The primary disadvantage of this approach is the electromagnetic interference (EMI) generated by the switching on-off action. The switching frequency in the limit cycle control would be determined by the net bus capacitance: the larger the capacitance the lower the switching frequency. The inertial energy storage element, considered primarily a "mechanical capacitor," would present an effective, large capacitance on the bus and thus provides a means for minimizing the switching frequency of the shunt regulator and attendant EMI.

Baseline Definition

The baseline design for a spacecraft power system configuration with inertial energy storage was defined in the initial studies to be a series type. This selected design is similar in configuration with the Multimission Modular Spacecraft Modular Power System (MMS/MPS) (Reference 12) and allows a basis for comparison with an electrochemical-based system (NiCd, NiH_2). The primary difference between the two systems is the bus voltage level (28 volts, MMS and 250 volts, baseline) and the power level (1 kW versus 2.5 kW). The baseline design configuration is shown in Figure 4 for reference.

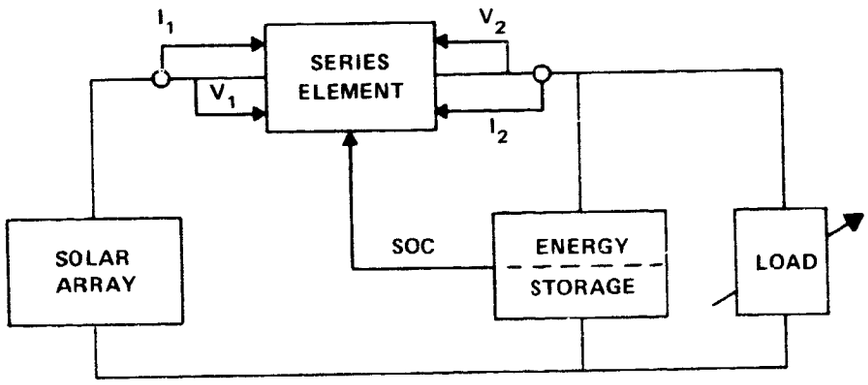

Figure 4. Baseline definition power system configuration.

Solar Array Characteristics

The available solar-array power in a given satellite depends on mission characteristics. Orientation to the sun, thermal extremes, and radiation damage are all factors that affect the solar-array output power. A typical example encountered in LEO missions is shown in Figure 5 for a sun-pointing application, curve A, and an earth-pointing application with a fixed array, curve B. These two cases indicate a significant variation in the amount of power that the power processing components and energy storage elements must be capable of handling. The curves shown are based on an energy balance condition and normalized with respect to the average load power. The power system configuration is the series type, as defined in the baseline definition. As can be seen from curve A, the peak power available from the array occurs at the beginning of the sunlight portion and is approximately 3 times the average load power. The average solar-array power is approximately 1.9 times the average load power. In contrast, the maximum power for curve B occurs during the middle of the sunlight portion and is approximately 4 times the average load power, yielding an average solar-array power of 2.6 times the load power.

The motor/generator design for the baseline definition is sized to handle a peak load of 3 times the average load power; consequently, the motor can handle the available power from either curve A or

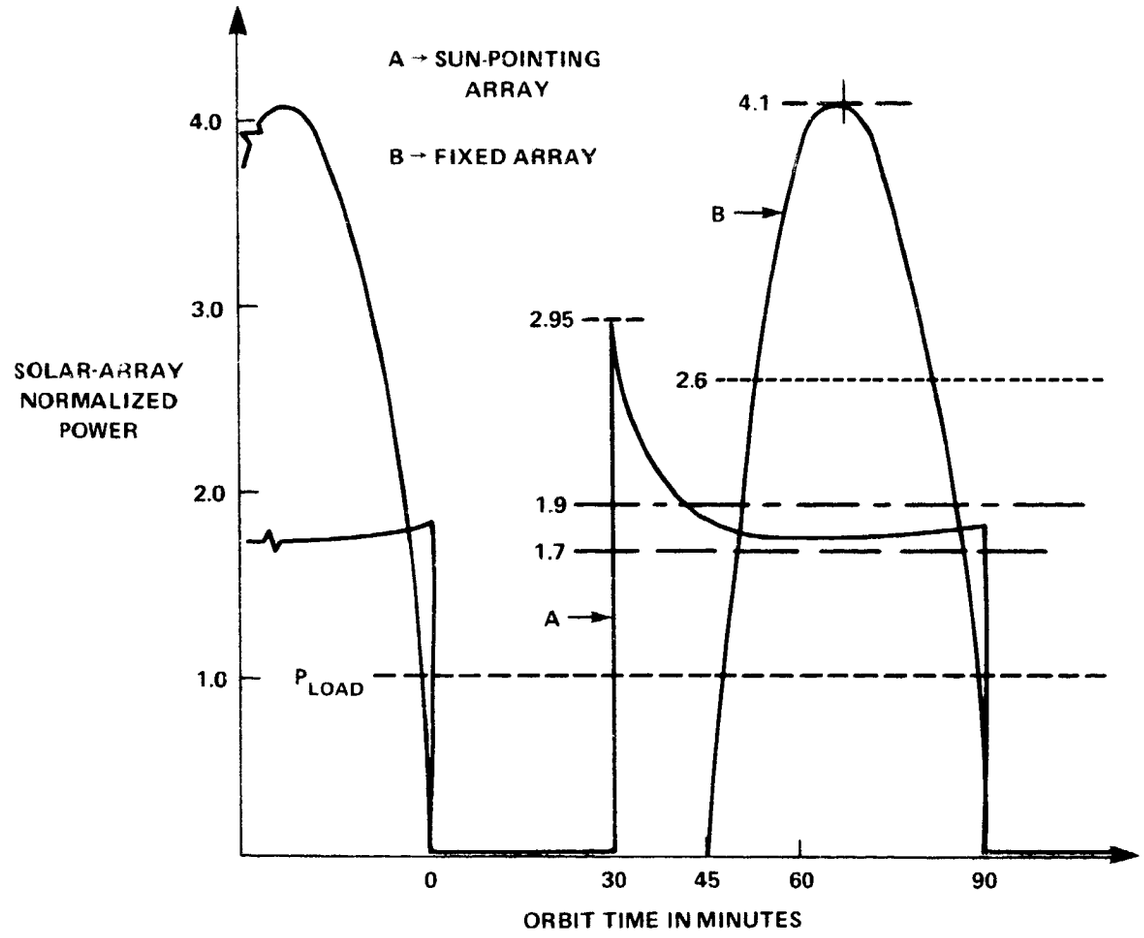

Figure 5. Solar array power profile.

or B. In contrast, the series element must be designed to handle 4 times the load power for curve B. If the series element is bypassed and the bus is operated at a fixed voltage, then for curve A the extracted power from the array will be approximately 1.7 times the average load power for an energy balance condition (same-size array). If, however, the load bus is allowed to change in proportion to the state-of-charge of the energy storage element, less power is extracted from the array and thus a larger array is required. The inertial energy storage element can be controlled to provide a constant voltage during charge (and discharge) and thus lends itself to this application.

Power Conditioning

Power conditioning, as it applies to a spacecraft power system, usually encompasses all other electrical aspects of the system that are required to interface with the energy source and energy storage elements. This would include passive as well as active devices, but the most significant function is generally the control of power to maintain energy balance. Within the defined baseline design, as shown in Figure 4, the series element provides the control of power from the array to the combined

load and battery. To adequately perform its function, the series element must sample the input voltage and current as well as output voltage and current; for an electrochemical energy storage element, it must sample battery voltage and temperature at a minimum. To provide flexibility, the series element would require additional inputs such as battery current and commands such as battery charge control mode (voltage-temperature taper or current control) on battery charge level (VT levels or current levels). An example of such a component is the Standard Power Regulator Unit (SPRU) in the MMS power subsystem (Reference 13). The SPRU samples the array voltage and current in order to peak-power-track the solar-array power variation as a function of temperature and also samples the battery voltage and temperature in order to provide voltage-temperature charge control in response to the commanded levels. Alternatively, it samples the battery current in order to provide battery charge control by battery current rather than by battery voltage-temperature (mode selection by command).

For the inertial energy-storage power system as defined in the baseline design, the series element would be required to sense array voltage and current in order to peak-power-track, sense output voltage to limit the bus voltage to an established upper level, and limit the output current for protection of its internal switching devices (semiconductors and magnetics). This simplifies the design (and interface) of the series element in that commands would not be required. Wheel speed is the only parameter required to determine and control the state-of-charge of the inertial storage element, and with a permanent magnet (PM) motor, the wheel-speed upper limit can be controlled simply by limiting the output voltage (bus voltage) of the series element to an upper limit. However, since differential wheel-speed control will be required to minimize attitude control disturbances, a separate power conditioning function must be accomplished. This power conditioning function can be performed within the electronics required for the PM motor/generator. The PM motor requires commutation to convert the inherent ac voltages (3 ϕ) induced in the static windings to the dc interface. To accomplish this, the typical configuration used is shown schematically in Figure 6. Transistors Q_1 through Q_6 are turned on or off in accordance with rotor position in such a manner as to accelerate the wheel in the motoring mode (during charge), and diodes D_1 through D_6 provide commutation during deceleration (during discharge). Speed control can be achieved by pulsewidth

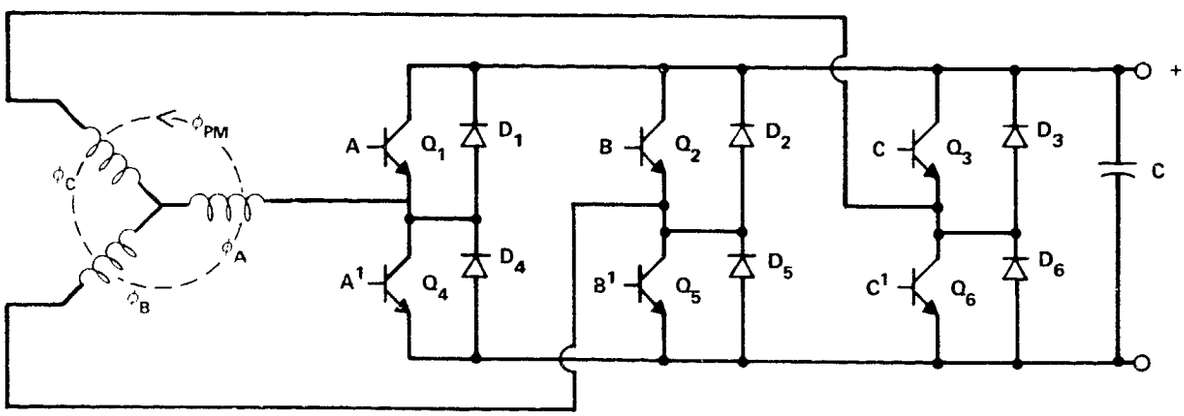

Figure 6. Schematic, motor/generator power electronics.

modulation of transistors Q_1 through Q_6 during charge or discharge, provided the inherent inductance of the stator windings can be effectively used in conjunction with capacitor C to perform the energy storage functions normally provided in high-frequency switching regulators. The equivalent circuit of this system can be represented as shown in Figure 7. Switch S_1 represents the switching action of transistors Q_1 - Q_6 and D_1 - D_6, with an effective duty ratio dependent on the ratio of bus voltage e_B and motor voltage e_m. Inductance L_m represents the effective stator winding inductance, and capacitor C absorbs the pulsating current. Power flow can be in either direction. For power flow from the bus to the motor, the equivalent power topology is commonly called a "buck" regulator, and for power flow from the motor to the bus, the power topology becomes a "boost" regulator. Switch S_1 can be realized as a combination of two transistors and two diodes, as shown in Figure 8.

For power flow from the bus to the motor, transistor Q_1 is controlled at the appropriate duty cycle and works in conjunction with diode D_2, whereas for power flow from the generator to the bus, transistor Q_2 is controlled and works in conjunction with diode D_1. The power MOSFET approaches

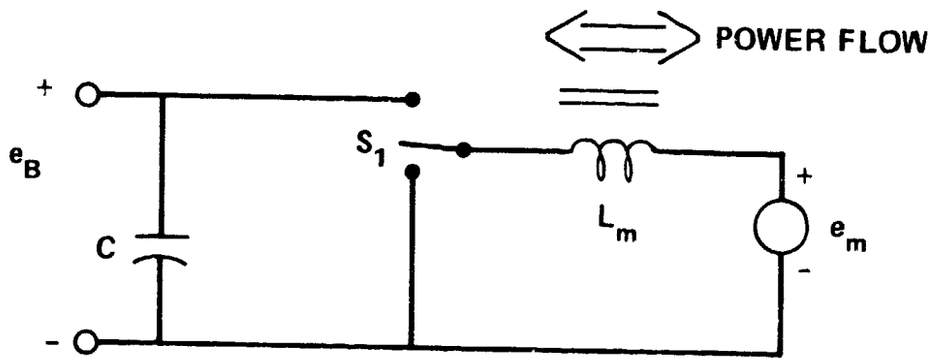

Figure 7. Equivalent circuit configuration for motor/generator electronics.

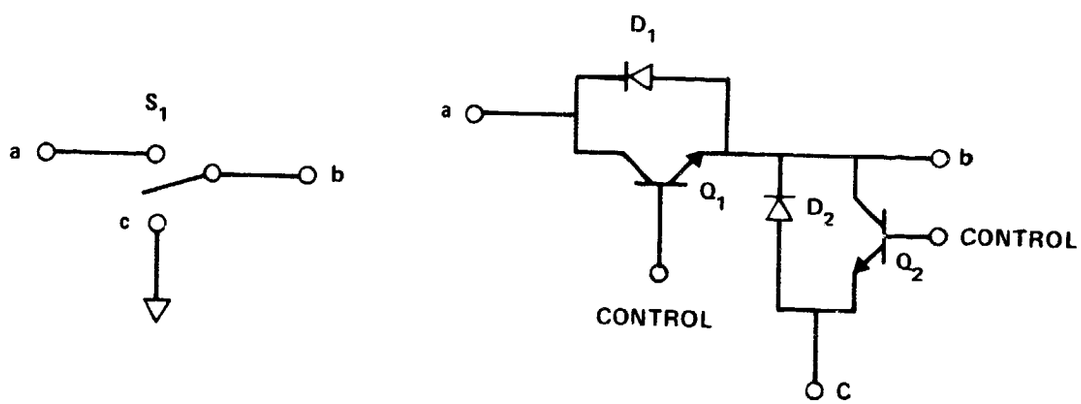

Figure 8. Transistor/diode configuration for switch realization.

the ideal characteristics required for realizing this equivalent switch because of the integral diode that exists from Drain to Source. Power MOSFET's with voltage ratings of 400 volts and current ratings of 10 amperes are presently available from various manufacturers. These devices feature fast switching, low-drive current, ease of paralleling, no secondary breakdown, and excellent temperature stability. They would be the first choice for the required switching devices within the power conditioning components defined as the series element and motor/generator electronics.

The corresponding wheel-speed change for a DOD of 75 percent is approximately 2 to 1; therefore, the induced motor/generator voltage will change 2 to 1. For a bus voltage of 250 volts, the induced motor/generator voltage would range from 200 to 100 volts, which imposes a duty-cycle range from 80 to 40 percent, well within conventional pulsewidth modulation techniques.

For the system configuration shown in Figure 3, the functions of peak-power-tracking and bus regulation are all accomplished within the motor/generator power electronics, thus eliminating the series element in the baseline definition at the expense of added complexity and increased rotational losses in the energy storage element. The power electronics or power conditioning required to do this is doubled. That is, the configuration shown in Figure 6 is repeated, thus requiring two sets of windings on the stator and two sets of transistor/diode switches. One set would interface directly with the solar array, and by pulsewidth modulation of the switches, the loading on the array can be controlled for peak-power-tracking, whereas pulsewidth modulation of the second set of switches/diodes provides a regulated bus to the load. This is analogous to a "buck" regulator connected between a solar-array source and a motor for the first set of power electronics and a "boost" regulator connected between the generator and the load.

Attitude Control System Compatibility

Any force tending to rotate the spacecraft away from its nominal attitude is considered a disturbance to the attitude control system (ACS) of the spacecraft. Disturbance torques are categorized as either cyclic or secular: Cyclic disturbances are defined as those that repeat over the course of succeeding orbital revolutions, causing no net change in attitude after one complete orbit, whereas secular torques are those that operate more or less constantly in the same direction and eventually require the use of thruster propellant to remove their cumulative effects after a certain number of orbits. Thrusters (gas jets) and angular momentum are the two basic techniques used to stabilize a spacecraft. A rotating body of any size has angular momentum, which is proportional to its size, and is measured by its moment of inertia times its angular velocity, having both direction and magnitude. Mathematically, the angular momentum magnitude is expressed as

$$H = I\omega$$

where

I = moment of inertia

ω = angular velocity

and its direction coincides with the spin axis under steady-state conditions.

The magnitude of the disturbance angular momentum of an energy storage wheel can be approximated by the following relationship:

$$\epsilon = \frac{1}{2} I\omega^2$$

where ϵ is stored energy. Solving for its moment of inertia, I, yields

$$I = \frac{2 \times \epsilon}{\omega^2}$$

and substituting in the mathematical relationship for angular momentum gives

$$H = \frac{2 \times \epsilon}{\omega}$$

The MMS uses momentum wheels with a momentum capacity of 20 N·m·s and a payload power capacity of 1.2 kW. The energy storage required by the power system in a LEO would be

$$\epsilon_m = \frac{P_L \times T_E}{DOD \times \eta_f}$$

where

P_L = payload power

T_E = eclipse time

DOD = depth of discharge

ϵ_m = maximum energy storage

η_f = round-trip efficiency

Using a DOD of 75 percent, an eclipse time of 30 minutes, and an efficiency of 80 percent yields

$$\epsilon_m \cong \frac{1.2 \times .5}{0.75 \times .8} = 1 \text{ kWh}$$

Solving for the angular momentum corresponding to this level of energy storage yields

$$H = \frac{2 \times 1 \text{ kWh} \times 3.6 \times 10^6}{2000} = 3600 \text{ N·m·s}$$

for an assumed angular velocity of 2000 radians/second.

This represents more than two orders of magnitude when compared with the momentum wheels of the ACS for MMS (20 N·m·s).

For kinetic energy storage compatibility with the ACS, the angular momentum vector must be cancelled to a level that is not considered a disturbance. Since the concept of inertial energy storage for spacecraft is based on two counterrotating wheels, the net disturbance will be

$$H_D = I_1 \omega_1 - I_2 \omega_2$$

where

I_1 and I_2 = moment of inertia of each wheel

ω_1 and ω_2 = angular velocity of each wheel

For a net zero disturbance, the spin axis of both wheels must be in exact alignment, and both wheels need to spin at exactly the same speed for identical moments of inertia. Any real system will have a misalignment of the axis and unequal moments of inertia, which leaves wheel speed as the simplest variable for controlling the net disturbance.

For comparison (using the MMS), two counterrotating wheels with an energy storage capability of approximately 0.5 kWh would be required, and the resulting disturbing momentum would be

$$H_d = 2\left(\frac{\epsilon_1}{\omega_1} - \frac{\epsilon_2}{\omega_2}\right) \approx (2 \times .5)(3.6 \times 10^6)\,\frac{(\omega_2 - \omega_1)}{\omega_1 \omega_2}$$

$$= 3.6 \times 10^6 \times \frac{(\omega_2 - \omega_1)}{\omega_1 \omega_2} \text{ N·m·s}$$

For a speed differential of 1 percent,

$$H_d = 3.6 \times 10^6\,\frac{(\omega_2 - 0.99\,\omega_2)}{0.89\omega_2 \omega_2} = \frac{3.6 \times 10^6 \omega_2}{\omega_2^{\,2}}\left(\frac{0.01}{0.99}\right)$$

$$= \frac{3.6 \times 10^6}{\omega_2} \times \frac{1}{99} \cong \frac{3600}{2} \times \frac{1}{99} \cong 36 \text{ N·m·s}$$

This disturbing torque represents twice the angular momentum capability of the momentum wheels in the ACS, and to further reduce the disturbance would require a differential wheel-speed control of approximately 0.005 percent for a 1-percent disturbance.

Thermal Control

Unless the wheel composite material is found to be sensitive to temperature extremes, there are no special requirements for thermal control in the application of the inertial energy storage element. Most of the heat dissipated will be located in the stationary nonrotating elements, thus allowing heat removal by thermal conduction. Temperature extremes between -25° and +50°C are within the capabilities of the electronics/generator.

Prelaunch Operations

The energy storage element baseline design is based on a hard vacuum environment for the energy wheels to operate at the high speeds without excessive drag and corresponding temperature rise in the rotating mass. This implies that either the module must be hermetically sealed and evacuated or the power system at the spacecraft level can only be successfully tested when the spacecraft is within a thermal vacuum chamber. The latter limits the amount of testing that can be accomplished at the spacecraft level especially during prelaunch tests. Therefore, a hermetically sealed enclosure for the energy storage element will be essential for satisfying typical ground testing requirements of the spacecraft. This enclosure may be achieved as a byproduct of the containment required for safety.

Launch Restrictions

Vibration and acceleration levels experienced during launch will require the wheels to be nonrotating, which will prohibit spacecraft operation unless an alternate power source or energy storage element is used. For shuttle launch operations, power will be available from the Space Transportation System (STS) bus (28 ±4 volts), and spinup can be performed before deployment.

Safety

As with any storage element, the potential for uncontrolled, sudden release of the stored energy can be hazardous. Specific containment requirements will depend on the intended application, that is, safety restrictions for manned vehicles during actual use and system impact on unmanned vehicles. Containment design is unique to the wheel design and wheel properties. Mass penalty for containment has been estimated between 25 to 100 percent of the rotating mass.

ENERGY STORAGE ELEMENT

Conceptual Design

The concept of the "Mechanical Capacitor" is documented in various reports (References 1 through 6), and its application in a spacecraft power system is further explained in Reference 14. The basic

concept under study is two counterrotating energy storage wheels with a small ID/OD ratio, magnetically suspended within the inner radius and accelerated/decelerated by a PM ironless armature, brushless motor, all fully enclosed to maximize volumetric efficiency.

A conceptual three-dimensional drawing of the module is shown in Figure 1. The design is a departure from the conventional flywheel systems that have been built and tested by the absence of a shaft to mechanically couple the flywheel to the motor/generator. The design depends heavily on magnetic suspension to maintain the rotating mass within acceptable clearances between rotating and stationary elements. The high rotational speeds necessary for energy storage (30,000 rpm) induce correspondingly very high speeds (800 m/sec) at the interface between the rotating and stationary parts. Approximate dimensions for the baseline design indicate an outer diameter of approximately 60 cm and a height of approximately 40 cm.

Critical Technologies

Critical technologies within the energy storage element are prioritized in the following manner:

- "Thick Rim" Wheel Development
- Magnetic Suspension
- Motor/Generator
- Containment
- Momentum Control

Specific details of each technology are further described in the following sections.

Wheel Development

Flywheel development, prompted by the energy shortage and stimulated by an organized effort of the DOE, has resulted in many approaches being brought to the testable model stage. The Lawrence Livermore National Laboratories (LLNL's), under contract with the DOE, narrowed their selection to three promising candidates:

- The cruciform spokes by Garret-Airresearch
- The laminated disk and rim by LLNL and the General Electric Company
- The woven spiral by AVCO Corporation

Of these three, only the woven spiral by AVCO exhibits a desirable form factor providing an essential monolithic "thick rim" with excellent volumetric efficiency and an ID/OD ratio sufficiently low

to support an integral motor/generator at an acceptable stress level. Unfortunately, development problems remain in the fabrication and curing of this design, and the DOE program is now facing termination. Some testing of sample wheels of this design by LLNL is still planned. The other two designs, although successfully tested (with the Garrett-Airresearch wheel found to exhibit a burst energy density of 80 Wh/kg), are not applicable to the integral design concept.

Telephone conversations with Mr. Anthony Coppa of the General Electric Company revealed a proposed wheel design that meets the essential properties of the "thick rim," and some discussions for fabrication and test at LLNL have been initiated.

A best rim design of the "thick rim" wheel for the "Mechanical Capacitor" is reported in Reference 4. This design used graphite-epoxy material with prestressing techniques and was sized for 10 kWh. Although the wheel was not fabricated and thus test results are not available, the design presents a third-potential wheel.

Other possible wheel designs may exist and prove to be superior in performance but have not been reported in the literature. Cost consideration was a large factor in the wheel development program sponsored by the DOE, primarily because of its intended application and economic factors. Boron fibers exhibit high-strength characteristics and, if combined with the proper matrix, although perhaps not economically feasible for terrestrial applications, may prove to be acceptable for space flight applications.

Development of fabrication techniques, achievement of balance specifications at least as good as commercial practice for equivalent high-speed rotating machinery, maintenance of balance within specification over a range of temperatures, and 10^5 cycle lifetime are all specific areas that must be addressed and verified. Some discouraging facts emerged in 1981, when wheel balance of composite wheels as currently being manufactured was reported in Reference 28. These were an order of magnitude worse than typically machined, high-speed rotating equipment and were not stable with time and cycle life.

Magnetic Suspension

Magnetic suspension is relatively new, but considerable developments have been reported in the literature. Magnetic bearings for the suspension of a 1-kWh flywheel system have been successfully designed, tested, and reported in References 17 through 18. Magnetic bearings as applied to flywheel systems are reported in References 19 through 22, and work on magnetic bearings in general is found in References 23 through 27. Wheel unbalance will determine the continuous dynamic load that the bearings must be designed to accommodate.

Calculations of the required mass for the baseline design of 2.5 kWh indicate a much higher mass than originally anticipated, placing additional requirements on the magnetic suspension. However, the detailed design will still depend on the wheel development.

Motor/Generator

Significant advances have been made in PM motor/generators using samarium cobalt magnets, electronic brushless commutation, and ironless armatures. This technology is well advanced as evidenced by the numerous reports (References 29 through 35). No serious problems are anticipated in the detailed design other than those caused by the magnetic suspension and wheel developments.

Containment

Successful containment design is based on the failure mode and postfailure phenomenon of the wheel, and the development of an analytic methodology. The LLNL plans to terminate the study of containment of flywheels during the fiscal year 1983 activities. A low-cost flywheel containment for vehicle application was designed by the General Electric Company, Space Systems Division, under subcontract with LLNL, and is documented in Reference 36. The total weight of the flywheel, housing, containment ring, and vehicle attachment ring is within the weight allowance set by LLNL and yields an overall energy density of 8 Wh/kg for a 0.25-kWh flywheel rotor. Significant progress was made toward a better understanding of composite rotor containment processes and how to design relative to them in response to direct burst action. Little understanding exists of axial burst and debris confinement effects in relatively small volume, low weight housings.

Brief discussions with Dr. Satish Kulkarni of LLNL on containment mass led to an estimate of 50 to 100 percent of the rotor mass, and more optimistically, discussions with Mr. Anthony Coppa of the General Electric Company indicated estimates as low as 25 percent. Specific containment requirements will depend on whether the application is for manned vehicles or for unmanned vehicles.

Momentum Control

Speed control of each wheel in a counterrotating pair module can be controlled by pulsewidth modulation of the power transistors required for armature commutation during charge (motor) and by pulsewidth modulation of shunt power transistors during discharge (generator), provided the self-inductance of each phase is sufficient to limit the current per phase to an acceptable value. An adequate reference signal will be required for differential speed control, and thus net zero momentum bias, and must be provided either by the ACS or within the power system for complete independence. Alternatively, the differential speed control can be used to provide attitude control functions. Based on preliminary calculations, speed control within 0.005 percent is required for a 1-percent momentum disturbance on the ACS.

Preliminary Design Calculations

Motor/Generator

The flywheel stores energy as kinetic energy. To provide an energy storage system that is an analog of a battery, it must include or be coupled with a motor and a generator. These elements provide the electrical-to-mechanical conversion and set the system power capacity. The dc motor is the

ideal choice to interface with a dc source (i.e., solar array). It offers the minimum weight (approximately 2:1 over ac motors) at a given efficiency and operating speed and operates with equal facility as a generator. The high speeds inherent in flywheel energy storage are helpful in reducing the mass of the motor/generator. The armature mass is inversely proportional to the square of the operating speed for given power and efficiency level.

The clear selection of a dc motor depends on electronic commutation that has removed the life and speed limitations of brush commutation. This also eliminates a source of drag which would be significant at high speeds. High-speed motor commutation demands the fast switching rates of which solid-state devices are capable and are only now becoming available at the power levels required by the system under consideration.

Two types of dc motors might be considered: series or shunt. The former offers constant voltage over a range of operating speed, whereas the latter is most efficient at a given operating point since the field excitation can be provided by permanent magnets at no extra cost of power. For the 2:1 range of speeds selected, which allows extraction of 75 percent of the stored energy, the permanent magnet type was selected, minimizing the weight and complexity of the motor/generator.

Rotational losses of the motor/generator are the major factors determining storage efficiency since it is a parasitic loss regardless of load demand. In order to minimize this loss, which in the conventional motor occurs primarily in the armature iron, an ironless armature (Reference 29) design was selected.

This type of motor has the armature winding in the airgap of the magnetic circuit and no stationary (armature) "iron" is used. The remaining parasitic loss is that produced by eddy currents within the armature conductors themselves. Although it cannot be totally eliminated, the effect can be reduced by the use of litz wire (each conductor is composed of insulated multiple strands).

One of the significant advantages of the motor/generator is that no "battery" of elements is required—the winding can be made to suit the voltage level desired. In fact, the generated voltage at a given operating speed also sets the torque developed per ampere for both motor and generator operation, regardless of any other motor parameter. This becomes the starting point for the motor design since the application sets the voltage and the flywheel design sets the speed.

For the baseline design, this was set at 300 volts at 3200 radians/second. The other basic design factor is armature resistance, which is set by the required electromagnetic conversion efficiency. In the baseline design, this must not be greater than 0.60 ohm. The permanent magnet has a linear speed-torque and current and generated voltage characteristic. The motor performance curves including efficiency are shown in Figure 9.

Since rare-earth cobalt magnets (Reference 37) provide the highest energy product of any known magnetic material and the best resistance to demagnetization, they are an obvious choice. In the most effective usage (facing the armature gap directly), they set the maximum magnetic flux density for the motor. The designer has some flexibility in selecting the length-diameter ratio of the motor. The motor field weight decreases with increasing diameter, but an upper limit is set by the

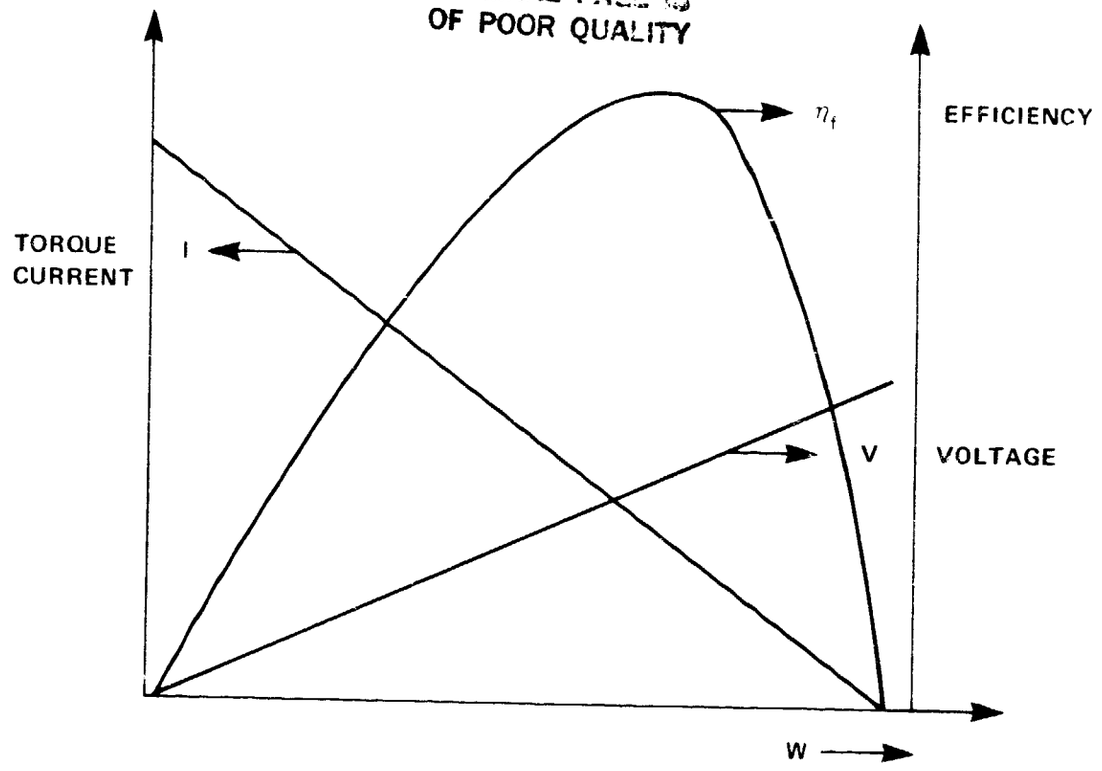

Figure 9. Typical dc motor characteristics versus speed.

centrifugal forces at high speeds. The weight of the field assembly also decreases as the number of poles increases. The upper limit is fixed by commutation frequency considerations. The number of pole pairs times the rotational rate equals the generated voltage frequency. For this case, 6 cycles by 510 rotations per second gives an internal operating frequency of 3060 Hz. The commutation rate for a three-phase full-wave commutator (Reference 38), selected as the best compromise of efficiency and complexity, is six times higher or 18.36 kHz. Control requirements by pulsewidth modulation or other switching technique would normally be at ten times this rate, which is considered to be state-of-the-art at this power level today. A motor of this power level would require about 1 kg on the rotating assembly and 1 kg on the stator for the essential electromagnetic parts. Therefore, a 3-kg total to also accommodate structural and thermal considerations is estimated to be feasible.

A motor/generator of this type will have a linearly varying output voltage dependent on wheel speed with an inherently ac-generated voltage that can be rectified with diodes or synchronously rectified. The specific circuit choices for commutation and rectification are discussed in the section on power conditioning. The source impedance of the motor/generator must be held to 0.60 ohm to meet the efficiency goals but may be reduced further to avoid thermal problems. The inductance of this type of motor is low but has not been estimated. It would be operated in a current-limited near-constant power mode with the charging rate set by the source capability and the discharge rate by the load during eclipse. There are no inherent cycle life limitations in the motor/generator other

than insulation degradation with time/temperature and the reliability of the commutation sensors and power electronics. Both of these, with adequate derating, can achieve $> 10^5$ hours. The electromagnetic efficiency of the motor/generator should exceed 95 percent in both the "charge" and "discharge" modes. Design emphasis therefore must be placed on minimization of the parasitic losses that are present over the whole charge/discharge cycle and that limit storage time to much shorter durations than electrochemical systems.

Magnetic Suspension

The magnetic bearing design is essential to the long life and high storage efficiency of the system. A multilevel four-quadrant suspension capable of providing 1.5 g's static radial load capacity to allow operational testing on the ground is considered essential. Dry-lubricated ball bearings capable of providing safe emergency coastdown without permanent degradation is needed in case of momentary power outages or dynamic overloads.

Two centrally located PM assemblies will be located above and below (axially) a central preloaded pair of ball bearings. Each assembly will provide a symmetrical torus of magnetic flux linking a magnetic cylinder that forms the inner core of the flywheel. An airgap flux level of 0.62 tesla over a total circumferential area of 264 cm^2 will be divided into four equal quadrants for radial control. A 50-percent peak-to-peak modulation of this flux level to control the radial position is required. Differential capacitive sensing of the rotors' nominal 0.012-cm clearance (0.120 magnetic radial gap) and four closed-loop servos will be required. Each of the four control loops must be capable of supplying a peak of 200 ampere-turns but will be operating in a nulling mode. Average power will depend on the degree of balance to which the flywheel assembly can be balanced and maintained during cyclic stress and life. The reliability of the system depends on the reliability of all the control electronics, sensors, and electromagnetic drive coils.

The following weight breakdown is slightly modified from the baseline design in the area of magnetic bearing weight allocations reflecting more recent design calculations:

Rotating Mass		Stator Mass	
Rim	30.0 kg	Housing	10.0 kg
Motor	1.5	Motor	1.5
Bearing	2.75	Bearing	6.0
Web	2.25		
Each wheel	26.5 kg	Each stator	17.5 kg
Dual flywheel assembly		108.0 kg	
Control and commutation package		12.5	
Containment (2) X 50% X 36.5 =		36.5	
2.5-kWh storage (5.4 kWh, peak)		157.0 kg	

Usable inertial energy storage density = 15.9 Wh/kg

Future Work

Unknowns

The concept of inertial energy storage for spacecraft is a new, relatively uncharted frontier. Although flywheels have been used for many years, this application requires an increase in the storage time constant by two orders of magnitude. To accomplish this requires reduction of parasitic (speed) losses especially if the motor/generator is integral (thus always rotating) with the flywheel. The rotational losses in the motor/generator (no-load) and in magnetic bearings at the required peripheral speeds have not yet been demonstrated. It is also mandatory to operate in a hard ($\leqslant 10^{-5}$ torr) vacuum, which implies a strong housing for ground testing.

The energy density necessary to be competitive with advanced chemical energy storage techniques mandates operating the flywheel near its ultimate strength, with all the hazards that entails. Modern fiber technology has provided the promise of attractive theoretical capability; however, the ability of composites to resist delamination and microscopic mass distribution changes under cyclic stress and environmental exposure is not known. Since these stresses are often perpendicular to the fiber direction, they are more affected by the matrix (typically epoxy) and the fiber-matrix bond than the intrinsic fiber properties. This makes them dependent on the fabrication and curing processes that are more difficult to control and monitor as the size and volume of the part increases.

In addition to the performance questions previously mentioned, the dynamic interaction of the dual-paired gyro in the context of the spacecraft environment must be explored. Although the gross dynamics of spinning bodies is well understood, the possibilities for interaction among many control loops and gyroscopic effects especially under fault conditions remain to be explored. A list of the evident unknowns is as follows:

- Composite fatigue behavior
- Composite balance and balance changes
- Control loop interactions
- Metal-to-composite interface
- High-speed magnetic losses
- High-speed motor losses
- Magnetic-to-ball bearing transition
- Weight of containment

Possible Solutions

Analytical work could serve to reduce the degree of uncertainty regarding the unknowns listed if a definite configuration is made available for analysis. Computerized tools for magnetic circuit analysis have been generated in recent years; however, considerable effort would be required to find the appropriate tools and to adapt them to this unique configuration.

The development and fabrication of high-energy density composite flywheels have been the subject of considerable research. Because of the dependence on batch fabrication for prototype manufacture, empirical data have been found essential to establish meaningful results. This extensive development and test program by the DOE is being terminated. Unless some of the current series of wheel developments can be used more or less directly, a considerable wheel fabrication and test program would have to be anticipated.

The use of analysis to reduce the uncertainty of design calculations assumes that all the "unknowns" are in fact recognized. It is believed that a correlated empirical hardware program would be needed to provide empirical data along with the analysis. In order to resolve the cost and hazard of experimental high-energy density storage system development, it was suggested that a one-quarter speed, one-sixteenth energy system be built, analyzed, and tested. This could provide a full-current (torque), low-voltage relatively safe and testable experimental version of the hardware and electronic control system. The extrapolation to higher speed performance could be done quite rigorously with laboratory instrumentation available to make detailed measurement of attitude controls interaction on simulators and of the electrical system behavior.

COMPARISON WITH ELECTROCHEMICAL SYSTEMS

A direct one-for-one comparison of a power system using inertial energy storage with a power system using electrochemical energy storage cannot be conducted primarily because of the lack of hardware data representative of inertial energy storage as compared with the available data of flight quality NiCd batteries. As new technology emerges and flight quality hardware is developed, the first approach generally taken is to fit the new hardware as a one-for-one replacement of the proven hardware, rather than to design a new system to enhance the characteristics of the new hardware, such as the application of NiH_2 cells in the Intelsat-V Satellite (Reference 39) and the Modular Power Subsystem for the Multimission Spacecraft (Reference 40). However, a comparison of some form is necessary to highlight the potential advantages and disadvantages of one over the other. Thus, the comparison of systems undertaken in this study is to compare the design of the system using available data on existing hardware and scaling it to fit the requirements.

Power System Configuration

Since the comparison conducted in this study is baselined for LEO applications, the system configuration is a series type using peak-power-tracking of the solar array for maximum power extraction. The system configuration, shown in Figure 10, is the same for all three energy storage elements (NiCd, NiH_2, and inertial) under consideration.

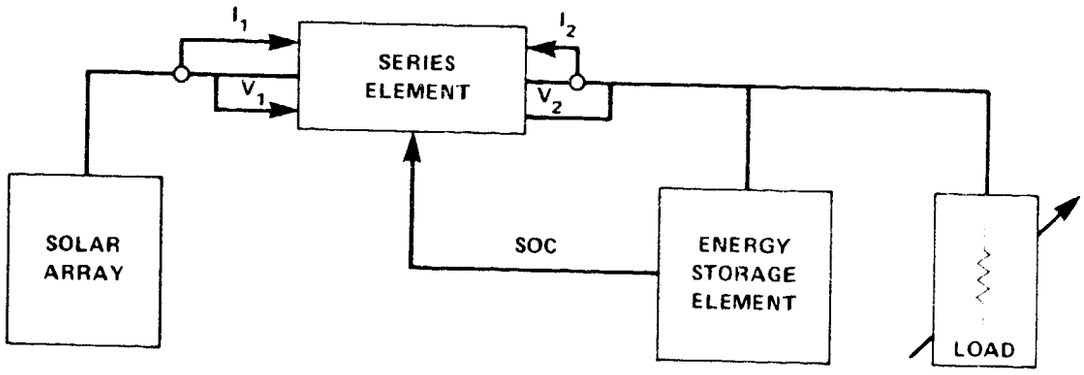

Figure 10. Power system configuration for comparison.

The key power processing component in this configuration is the series element since it provides peak-power-tracking and charge control. Other components usually found in the system, such as housekeeping functions, protection circuitry, and power distribution, are not considered in the comparison primarily because of similarity.

The system is sized for a payload requirement of 2.5 kW operational, 7.5 kW peak for 9 minutes, and a 30-minute eclipse, 60-minute sunlight orbit. This payload represents a factor of 2.5 times the MMS payload specification. The bus distribution voltage selected is 250 volts, nominal.

Power Flow and Energy Balance

For the system configuration selected and under comparison, the net in/out efficiency of the energy storage element determines the size of the prime energy source required for energy balance. An energy flow diagram for the system shown in Figure 11 is used as a basis for comparison. Energy numbers used are sized for the peak load that occurs during the eclipse portion of the orbit.

During the eclipse, energy required by the load is

$$E_{E1} = (2.5\ \text{kW})\ \frac{(30\text{-}9)\ \text{min}}{60\ \text{min}} + \frac{(7.5\ \text{kW})\ (9)\ \text{min}}{60\ \text{min}}$$

$$E_{E1} = 0.875\ \text{kWh} + 1.125\ \text{kWh} = 2.0\ \text{kWh}$$

and energy required by the load during sunlight is

$$E_{S1} = (2.5\ \text{kW})\ \frac{(60\ \text{min})}{60\ \text{min}} = 2.5\ \text{kWh}$$

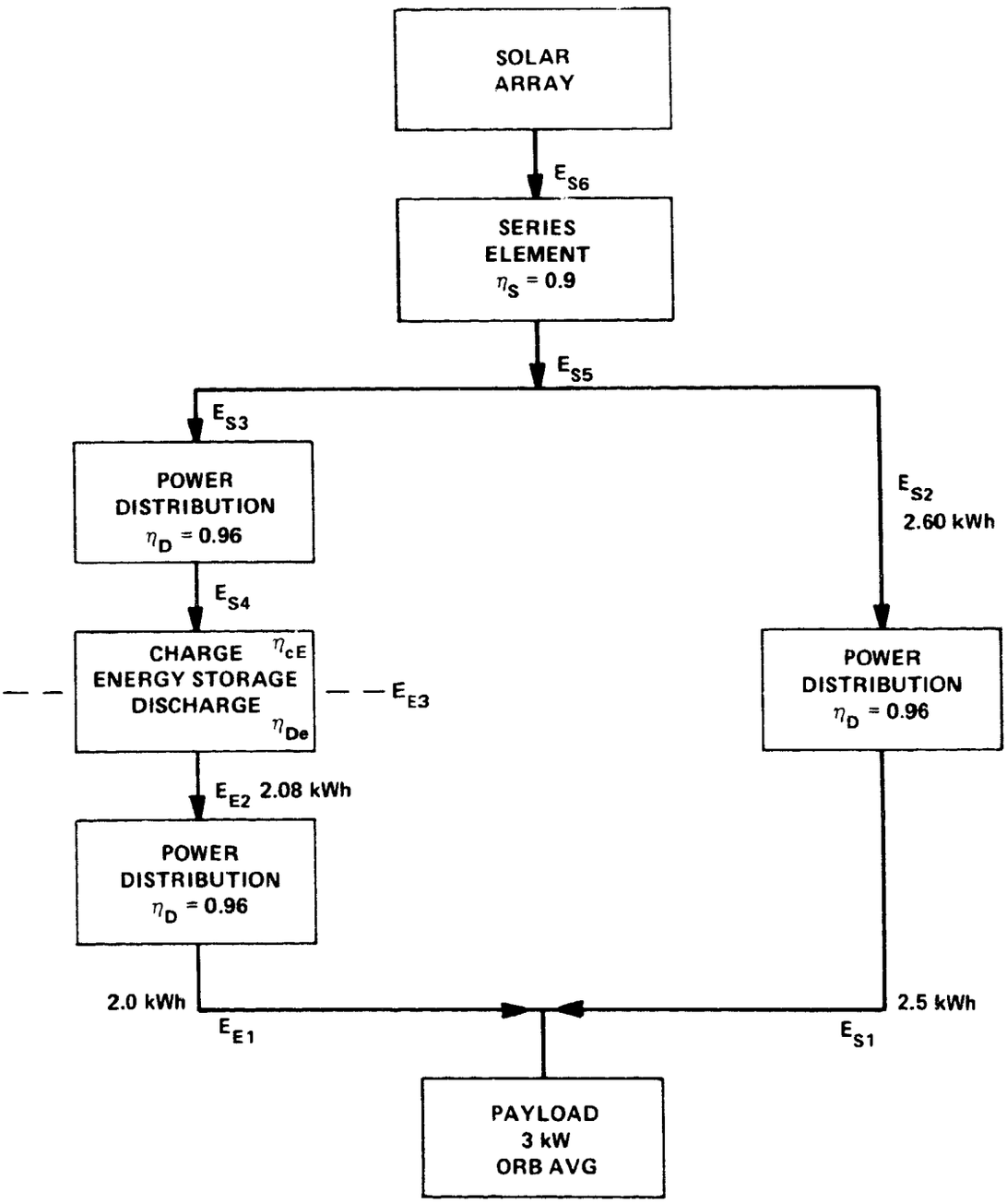

Figure 11. Energy flow diagram and energy balance.

Table 1 shows the various energy levels required for energy balance of the systems under comparison.

Table 1
Energy Flow Comparison

	E_{E2}	E_{E3}	E_{S4}	E_{S3}	E_{S2}	E_{S5}	E_{S6}	P_{SA}
Flywheel	2.08	2.33	2.61	2.72	2.6	5.32	5.92	5.92 kW EOL
NiH_2	2.08	—	2.6	2.71	2.6	5.31	5.91	5.91 kW EOL
NiCd	2.08	—	2.6	2.71	2.6	5.31	5.91	5.91 kW EOL

Detailed calculations and estimates for these energy levels are as follows:

1. Inertial Energy Storage

$$E_{E3} = \frac{E_{E2}}{\eta_{ge}\ \eta_g\ \eta_{fL}}$$

where

η_{ge} = generator electronics efficiency
= 0.95

η_g = generator efficiency
= 0.96

η_{fL} = flywheel system efficiency
= 0.98

$$E_{E3} = \frac{2.08}{(0.95)\,(0.96)\,(0.98)} = \frac{2.08}{0.894} = 2.33 \text{ kWh}$$

Similarly,

$$E_{S4} = \frac{E_{E3}}{\eta_{FL}\ \eta_m\ \eta_{mE}}$$

where

η_{FL} = flywheel system efficiency
= 0.98

η_{m} = motor efficiency
= 0.96

η_{mE} = motor electronics
= 0.95

$$= \frac{2.33}{0.894} = 2.61 \text{ kWh}$$

2. Electrochemical Energy Storage (NiCd, NiH_2)

$$E_{S4} = \frac{E_{E2}}{\eta_{DC}}$$

where η_{DC} represents the net discharge-charge efficiency, or

$$\eta_{DC} = \eta_{AH} \times \frac{V_D}{V_C}$$

where

η_{AH} = ampere-hour efficiency

V_D = average voltage during discharge

V_C = average voltage during charge

For a 25-percent DOD NiCd battery:

$$\eta_{AH} = \frac{1}{1.07}$$

$$\frac{V_D}{V_C} = \frac{1.25}{1.46}$$

$$\eta_{DC} = 0.8$$

For a NiH_2 operated at 40 percent, the same net efficiency is assumed; therefore, the energy required, shown in Table 1, is essentially the same for NiCd and NiH_2.

Electrochemical Energy Storage Data Base

Sizing of the NiCd and NiH_2 batteries for the system comparison is based on a data base compiled from existing battery designs for various spacecraft programs. This data base is given in Table 2. Although rated ampere-hour capacity was used for the energy capacity calculations, NiCd nominal Ah capacity is found to be 15 to 20 percent more. A reduction of the data contained in Table 2 when combined with inertial energy storage data is tabulated in Table 3 in an attempt to demonstrate the development of flight hardware from the theoretical state to the practical/usable state. The same data are displayed as a bar chart in Figure 12.

NiCd Battery Design

The size and quantity of cells required to meet the payload requirements for the selected system configuration, using NiCd cells, are calculated as follows:

1. Number of Cells

   For a nominal 250-V bus, a typical nominal cell voltage of 1.34 V/cell can be expected for a 25-percent DOD, 10°C application. Thus, the required number of cells is:

$$N_c = \frac{250}{1.34} = 187$$

2. Ah Rating

   Two factors must be considered in selecting cell size: maximum discharge rate and depth of discharge. Since the peak payload power is 7.5 kW, then

$$I_{DISCHARGE|max} \cong \frac{7500\ W}{250\ V} = 30\ \text{amperes}$$

   Limiting the maximum discharge rate to 3/4 C rate requires a 40-Ah rated cell. Conversely, for an average discharge voltage of 1.25 V/cell, the required Ah rating is

$$I_{AH} = \frac{2.08\ kWh}{(1.25 \times 187)(0.25)} = 35.6\ Ah$$

   Thus, for the application, a 40-Ah cell is selected as the required cell size, and 187 cells in series provide the necessary bus voltage.

   The corresponding weight for this battery is calculated from the data in Table 2 as follows:

   The TDRS battery uses twenty-four 40-Ah cells and weighs 41.9 kg, thus

$$W_\beta = \frac{187}{24} \times 41.9 = 326\ kg$$

Table 2
Aerospace Battery Data Base

	Cell Data		Number of Cells	Battery Weight		Total Energy Capacity (Wh)	Energy Density (Wh/kg)	
	Ah	Type		kg	lb		Total	Usable
Landsat-D (MMS)	50	NiCd	22	51	112	1375	27	6.7
TDRS*	40	NiCd	24	41.9	92.3	1200	28.6	7.2
NOAA-A	26.5	NiCd	17	25.3	55.7	563	22.3	5.6
SMM (MMS)	20	NiCd	22	23.8	52.4	550	23.1	5.8
ATS-6*	15	NiCd	19	17	37.4	356	21	5.2
OSO-I	12	NiCd	21	12.6	27.8	315	25	6.3
AE-C	6	NiCd	24	8.9	19.6	180	20.2	5.1
IUE*	6	NiCd	17	5.85	12.9	128	21.8	5.5
Intelsat-V*	34	NiCd	28	32.5	71.6	1190	36.6	9.2
Intelsat-V*	30	NiH_2	27	30.2	66.4	1045	34.7	13.9
MMS	50	NiH_2	21	50.3	110.8	1355	27	10.8

*Synchronous orbit

Notes: 1. Energy storage based on: 1.25V/cell NiCd
1.29V/cell NiH_2
Rated Ah capacity

2. Usable energy density based on: 25-percent DOD for NiCd
40-percent DOD for NiH_2

Table 3
Development of Energy Storage Elements

Electrochemical	Energy Density Wh/kg			Inertial
	NiCd	NiH_2	Inertial	
Theoretical	[illegible]	378	550	Theoretical
Cell (actual)	37	50-60	80	Rotor (actual)
Cell (rated)	31	41-52	45	Rotor (rated)
Battery (rated)	20-35	34-41	32	Flywheel (rated)
Battery (usable)	5-9	11-14	16	Flywheel (usable)

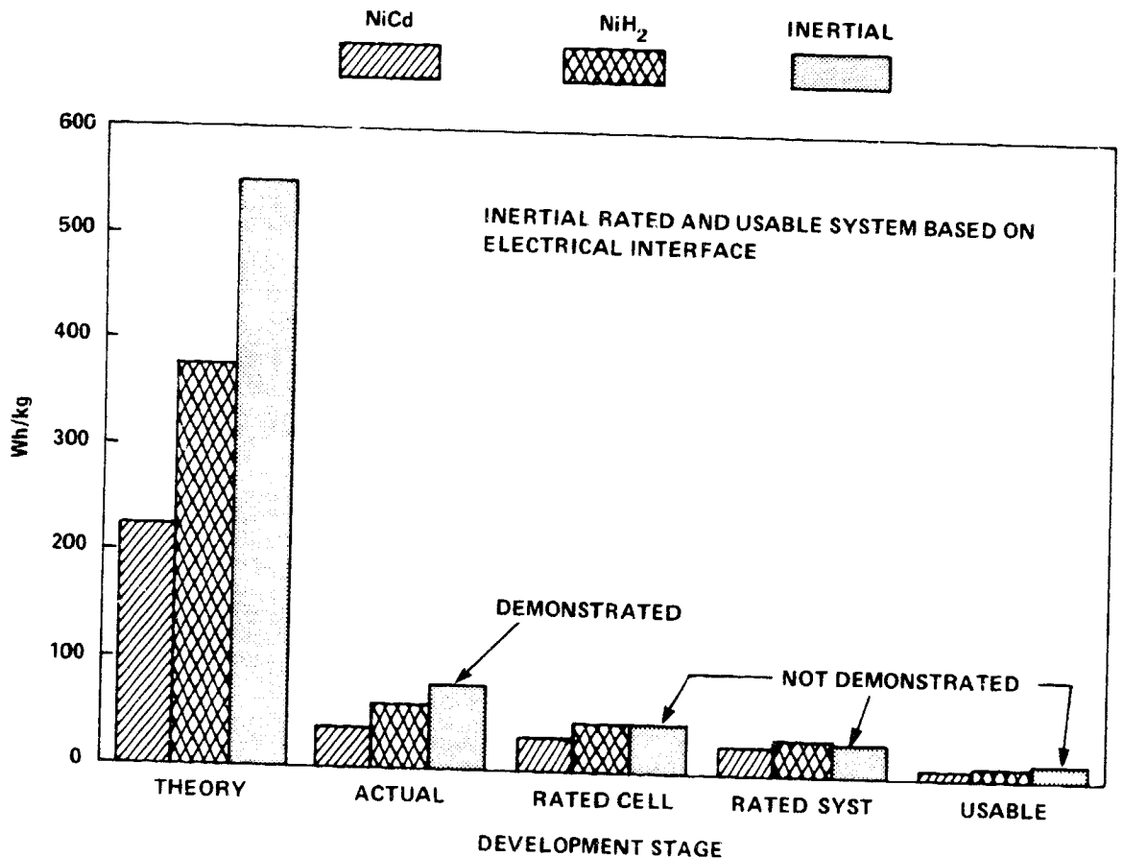

Figure 12. Development of energy storage elements (electrochemical and inertial).

The corresponding volume for this battery is scaled from existing battery dimensions by the ratio of cells required, or

$$V_{\beta} \cong 0.16\ m^3$$

The corresponding usable energy density is

$$\frac{2080\ Wh}{326\ kg} = 6.4\ Wh/kg$$

$$\frac{2080\ Wh}{0.16\ m^3} = 12\ kWh/m^3$$

NiH_2 Battery Design

The design of the NiH_2 battery is essentially the same as that of the NiCd. However, fewer cells are required since the volts/cell is approximately 40 mV higher; thus, the number of cells required would be

$$N = 187 \times \frac{1.34}{1.38} = 181\ cells$$

The Ah rating of the cell, using a 40-percent DOD as a guideline, would be

$$I_{AH} = \frac{2.08\ kWh}{(1.29\ V)(181)(0.4)} = 22\ Ah$$

Supplying the 7.5-kW pulse of power for 9 minutes during the eclipse means a discharge rate of 1.5C rate; applying a maximum discharge rate of C rate implies selecting a 30-Ah rated cell, such as the 30-Ah cell for Intelsat-V. The weight estimate based on this battery would be

$$W \cong \frac{181}{27} \times 30.15\ kg = 202\ kg$$

and the volume would be

$$V \cong \frac{181}{27} \times 0.52 \times 0.52 \times 0.22 = 0.4\ m^3$$

The usable energy density for this application is thus calculated as

$$\frac{2080\ Wh}{202\ kg} = 10.2\ Wh/kg$$

$$\frac{2080\ \text{Wh}}{0.4\ \text{m}^3} = 5.2\ \text{kWh/m}^3$$

Inertial Energy Storage Element

Estimates for the weight breakdown of the inertial energy storage element are as follows:

1. 50-Percent DOD

   The required energy storage from Table 1, $E_3 = 2.33$ kWh, rounded off to the nearest tenth, is 2.4 kWh.

   For 50 percent, each wheel must be capable of 2.4 kWh; for an attainable energy density of 45 Wh/kg, maximum operational speed, 10^5 cycles fatigue stress, requires a rim design weight of

$$W_R = \frac{2400\ \text{Wh}}{45\ \text{Wh/kg}} \cong 53\ \text{kg}$$

   Allowing a total of 5.75 kg for the motor rotor (1.5 kg), bearing rotor (2.0 kg), and webspokes (2.25 kg), the total rotating mass is 58.75 kg.

   The static or nonrotating mass would be:

   10 kg – Structure and housing

   1.5 kg – Motor stator

   4.0 kg – Bearing stator

   The subtotal weight for one energy storage element is thus 68.5 kg, and for the pair of counterrotating assembly, the total weight becomes 137 kg. Although this exceeds the original target goal of 115 kg, the usable energy density is ≈ 2080/137 = 15.2 Wh/kg.

   An approximate wheel size for this energy storage level is an OD of 0.44 m and height of 0.25 m, yielding an overall volume of

$$V = \frac{(0.44)^2}{4} \times 11 \times 0.25\ \text{m} \cong 0.04 \text{ and for two wheels}$$

$$V_T \cong 0.1\ \text{m}^3$$

   and

$$E_u/V_T = \frac{2080}{0.1} = 20.8\ \text{kWh/m}^3$$

2. 75-Percent DOD

For 75-percent DOD, the maximum energy storage capability would be 2.4/0.75 kWh or 1.6 kWh per wheel. Using an attainable energy density of 45 Wh/kg (at maximum operational speed, 10^5 cycles fatigue stress) requires a rim design weight of

$$W_R = \frac{1600 \text{ Wh}}{45 \text{ Wh/kg}} = 35.5 \text{ kg}$$

Using the same weight allocation for the motor/generator rotating mass as for the 50-percent DOD case, except allowing an increase of 10-percent weight estimate for the additional speed change, results in a rotating mass of approximately 42 kg. Similarly, the static mass would be 17 kg, yielding a total mass of 59 kg. For two counterrotating wheels, the total weight becomes 118 kg.

If allowance is made for containment, a preliminary estimate of 50 percent of the rotating mass is reasonable, yielding a weight estimate of 160 kg. This results in a usable energy density of 2080/160 kg = 13 Wh/kg, and without containment penalties, the usable energy density would be 2080/118 = 17.6 Wh/kg. Volumetric energy density would be approximately the same as the 50-percent DOD case, or

$$\frac{2080}{0.1 \text{ m}^3} = 20.8 \text{ kWh/m}^3$$

Voltage Regulation

Bus voltage regulation is one measure of system performance, and since the load is across the energy storage element, the bus voltage is primarily determined by the energy storage element. The extreme limits are set by the end-of-charge maximum voltage limit and by the minimum end-of-discharge voltage. For NiCd, the maximum allowable charge voltage is 1.52 V/cell (based on the GSFC VT level 8 at 0°C) and the minimum end-of-discharge voltage is 1.15 V/cell (end-of-life, 10°C, 25-percent DOD). For 187 cells in series, the voltage limits are 284 volts maximum and 215 volts minimum, or 250 V ±35 V. These limits represent a voltage regulation band of approximately ±14 percent, and a similar regulation band would be expected for the NiH_2 battery.

A simple analogy of the inertial energy storage element is to consider it as a capacitor. The delta energy stored and released is calculated as:

$$\Delta\epsilon = \epsilon_2 - \epsilon_1 = \frac{1}{2} C (V_2^2 - V_1^2)$$

for a 50-percent DOD (baseline design)

$$\Delta\epsilon = 0.5\,\epsilon_2 = \frac{1}{2} C (V_2^2 - V_1^2)$$

but since

$$\epsilon_2 = \frac{1}{2} C V_2^2$$

then

$$(0.5)\ \frac{1}{2} C V_2^2 = \frac{1}{2} C (V_2^2 - V_1^2)$$

$$V_1 = V_2 \sqrt{0.5} = V_2\,(0.707)$$

but

$$V_{NOM} = \frac{V_1 + V_2}{2} = \frac{V_2\,(0.707) + V_2}{2}$$

$$V_{NOM} = \frac{V_2\,(1.707)}{2} = 0.854\,V_2$$

for $V_{NOM} = 250$ V

$$V_2 = \frac{250}{0.854} = 293 \text{ volts}$$

$$V_1 = .707\,V_2 = 207 \text{ volts}$$

The delta voltage is 86 volts, or ±43 volts. Accounting for IR drops, a delta of ±50 volts would be expected. Thus, the voltage regulation for a 50-percent DOD inertial energy storage element would be 250 ±50 V or 250 V ±20 percent. However, since the counterrotating wheel speed must be precisely controlled, the motor/generator electronics will be required to perform an additional function besides commutation. Pulsewidth modulation will be used to control wheel speed in either the charge or discharge mode. This isolates the bus from the terminal voltage of the motor/generator and provides an additional control feature, bus voltage regulation. With this voltage regulation control feature, the wheel can be operated over a larger DOD, resulting in a more favorable energy density. Thus, for a DOD of 75 percent, it is anticipated that the bus can be regulated to within ±2 percent.

Power Processing Weight Estimate

In order to achieve an overall weight estimate for the power system comparison, some measure of weight allocation should be given for the series element.

The series element in this application must be capable of processing a maximum power of approximately 3 times 2.6 kW (from Figures 5 and 10) or 7.8 kW. The Standard Power Regulator Unit for the MPS/MMS is capable of an output power of approximately 3 kW and weighs approximately 17 kg. However, for operation at higher frequencies and higher voltages, a weight estimate of approximately 20 kg is not unreasonable.

For the system configuration consisting of a sequential switching shunt regulator and the inertial energy storage element (regulated bus system), a weight of 7 kg is estimated for the necessary electronics.

Solar Array Weight Estimate

The required power from the solar array is approximately 5.92 kW at EOL, as shown in Table 1, for the three systems. This represents a weight allocation of 106 kg based on 56 W/kg technology.

For the shunt configured system, the losses of the series element make up for the loss of peak power available at the beginning of sunlight. Thus, the required power is approximately 5.9 kW, and the weight allocation is the same.

Performance Comparison

The various parameters and characteristics discussed in the previous sections of this report are tabulated for comparison in Table 4. The parameters indicated for NiCd technology are based on known, real data, whereas those for NiH_2 are not as firm and those for the inertial energy storage technology yet remain to be verified. However, inertial energy storage offers significant improvement in lifetime, voltage regulation, and waste heat rejection (thermal constraints). Significant weight improvement can be realized for a 75-percent DOD wheel system without containment and in a shunt system configuration (35-percent reduction compared with NiCd; 30-percent reduction compared with NiH_2).

Standby power for the flywheel is expected to be significantly higher than that for the self-discharge of electrochemical energy storage systems. This does not significantly alter the efficiency of the system in a LEO application because of the relatively short times during which the energy storage element is left in the "open circuit mode." Specific applications, in which the energy storage element is left idle, or, in an open circuit mode, the flywheel system would not compare favorably with electrochemical systems.

Inertial energy storage offers improvement in usable energy density primarily because it is operated over a larger DOD in a cyclic fashion. This high DOD provides a small margin of energy storage in the event of system anomalies, whereas in comparison, the electrochemical system provides a higher reserve margin for anomalies. Voltage regulation suffers as soon as the stated DOD is exceeded for any system, but it becomes a survivability constraint and can be tolerated if being incorporated in the design.

Table 4
Comparison for 3-kW, 250-Vdc Spacecraft Power System

		NiCd	NiH_2	Inertial				
				50%[a]	75%[b]	75%[c]	75%[d]	75%[e]
Lifetime		5 yr 25% DOD	5 yr 40% DOD	20 yr based on 10^5 cycles, 90 min LEO orbit				
Thermal Constraints		0° to 20°C	0° to 20°C	-25° to +50°C				
Launch Constraints		None	None	Wheels must be locked (vibration level)				
Compatibility	ACS	No Interaction	No Interaction	Differential speed control of wheel speed required				
	Struct.			Unbalance causes vibration unknown amount				
Voltage Regulation		±14%	±14%	±2%				
Energy Density	Wh/kg	6.4	10	15.2	17.6	13	17.6	13
Energy/ Volume	kWh/m³	13	5.2	20	20	20	20	20
Charge Control		Complicated	Pressure sense may simplify detection and control	Wheel speed provides simple SOC detection and control method				
Weight Estimate in kg	Storage	326	202	137	118	160	118	160
	Solar	106	106	106	106	106	106	106
	Processing	20	20	20	20	20	7	7
	Total	352	328	263	244	286	231	273

[a] 50% DOD, differential speed control, no containment
[b] 75% DOD, differential speed control, no containment
[c] 75% DOD, differential speed control, containment allowance
[d] 75% DOD, differential speed control, no containment, shunt det
[e] 75% DOD, differential speed control, containment allowance, shunt det

The system weight estimate does not include estimates for harness and circuitry normally required for telemetry performance parameters such as voltage, current, temperature, and for bus protection, power distribution, and power system configuration (relays and power disconnect).

Reliability and cost are two subjects not tabulated in the comparison but certainly require discussion. Reliability in electrochemical energy storage is usually achieved by using two or more batteries with an attendant reduction in payload power in the event of a loss of one battery, or a reduction in lifetime because of the higher operating DOD. The use of 187 cells in series for a 250-Vdc bus poses some reliability hazards, and work around circuitry would be required, such as group of cells voltage sensing, cell bypass techniques, and some form of cell reconditioning.

Reliability of the inertial energy storage element will depend heavily on conservative design stress levels to ensure the 20-year lifetime and also depends on electronic circuit reliability of the magnetic bearing and motor/generator electronics. With two counterrotating wheels for energy storage, the loss of one wheel implies the loss of both because of the resulting momentum interaction with the ACS.

The manufacturing cost of an inertial energy storage system should be competitive with the cost incurred in the manufacturing and testing of flight quality aerospace cells. For example, the cost to build, test, and deliver a flight quality 50-Ah 22-cell NiCd NASA standard battery is approximately $176,000 (in 1982 dollars), that multiplied by 187/22, approximately $1.5 million, would be the cost for the battery required in this study, and represents nonrecurring cost. Similarly, once the manufacturing methods have been established for the inertial energy system, it would be reasonable to expect that a complete system, built and tested, should cost approximately $600,000.

CONCLUSIONS

The application of inertial energy storage for a spacecraft power system relies on the key characteristics of the energy storage element. Power distribution (ac versus dc), power system configuration, performance, and system compatibility have been evaluated on the basis of the conceptual flywheel system design (developed at GSFC and referred to as the "Mechanical Capacitor") consisting of two counterrotating composite rotors, suspended magnetically at the inner diameter and accelerated/decelerated by a PM brushless, ironless dc motor/generator contained within the stationary inner volume. This energy storage element exhibits characteristics similar to those of an electrochemical energy storage element, which makes it an almost one-for-one replacement. AC power distribution is not found to be advantageous since the inertial energy storage element does not exhibit the desirable characteristics required by an ac power distribution system. The power system configuration selected is identical with state-of-the-art systems using electrochemical energy storage. A unique system configuration identified incorporates the main functions of power conditioning within the energy storage element, reducing the system component count from three to two, namely solar array (1) and energy storage (2). Performance is highlighted as long lifetime (20 to 30 years), high temperature waste heat rejection, simple state-of-charge detection and control, inherent high-voltage implementation, high-pulse power capability, higher energy density (Wh/kg) than NiCd, and higher volumetric density than NiH_2 (Wh/m^3). These features, although potential, make inertial energy storage a significant improvement over electrochemical systems. Compatibility with other

systems is found to be adequate, with the recognition that momentum disturbance to the attitude control systems must be precisely controlled or alternatively used for attitude control as well.

Self-discharge, or energy storage efficiency, containment, and launch restrictions are three areas that require careful consideration in the intended application. For example, in LEO applications the self-discharge of the inertial energy storage element does not significantly affect the overall system performance. In unmanned vehicles, containment requirements would be less demanding than in manned vehicles. Spacecraft acquisition during launch may require electrochemical energy storage in a launch mode in which the energy storage wheels must be "locked."

Combined application of inertial energy storage and attitude control functions has been the focus of attention in two reported studies; one by NASA/Langley Research Center (LaRC) in 1974 (Reference 41) and the other by the European Space Agency (ESA) in 1978 (Reference 42). Both reports find the combined functions to be feasible and result in conceptual designs and methods to accomplish the objective. The NASA/LaRC study effort progressed to the development of inertial energy storage hardware using titanium for the wheel and conventional bearings. The ESA study has not proceeded to the development of hardware but identifies the merits of magnetic bearings and composite rotors. In either case, the subject of inertial energy storage for spacecraft application remains a "study" effort, and until competitive hardware is developed, its application will remain on paper. Since the inertia required for energy storage is significantly larger than that required to perform attitude control functions, a conservative program (and lower risk) to undertake is to develop the fundamental inertial energy storage hardware. Once developed, the hardware application will follow; for if it is to be used in power systems, it must be controlled; and if it must be controlled, it should be used for attitude control as well.

The mechanical capacitor conceptual design considered in this feasibility study is based on three key technologies, two of which are well developed and have been demonstrated, but yet remain to be used in flight hardware. These two technologies, magnetic bearings and dc PM ironless armature, brushless motors, ideally suited for use in momentum wheels for attitude control, do not exist in the list of flight-approved hardware. Conventional bearings and ac motors, presently used in most momentum wheels, do not offer the high performance required for an inertial energy storage system to be competitive with electrochemical systems. Conceivably, if a flywheel system as conceptually described in this report can be successfully demonstrated, it would facilitate or encourage the use of these two technologies in momentum wheels. On the other hand, if these two technologies existed in present flight hardware, a significant data base would have been available to substantiate the feasibility of inertial energy storage. However, the key single most critical technology is the high-speed composite rotor, which, although significant progress has been achieved within the last two years, requires further development, verification, and system implementation.

In terrestrial applications, inertial energy storage becomes competitive over electrochemical systems from a "maintenance free" consideration. Similarly, in spacecraft applications, long lifetime is the key advantage of inertial energy storage over electrochemical storage. To realize this, successful integration of the critical technologies identified in this report must be pursued.

During the last few years, flywheel technology was supported primarily by the Department of Energy, but it is now approaching termination. Recent results obtained by the General Electric Company under this program are very encouraging in that they support the assumptions used for energy density capability in this study. In addition, results on cyclic testing have verified 10^4 cycles, which is one order-of-magnitude improvement over past performances and approaches the potential cycle life of 10^5 cycles referenced in this report.

RECOMMENDATIONS

Significant potential advantages of inertial energy storage for spacecraft power systems as identified in the conclusions warrant the development of hardware to a proof of principal stage. To accomplish this, a sizable commitment in resources is required to demonstrate a complete power system. At a minimum, the development of a suitable composite rotor should be pursued with less risk involved at the expense of a longer time span in achieving the proof of principal hardware. Magnetic suspension and motor/generator development should be accomplished together, following demonstration of a successful rotor design. Verification of the fundamental energy storage function would occur when the rotor, suspension, and PM motor/generator are integrated as one. After the energy storage function has been demonstrated, the next step would be attitude control compatibility verification. The development and demonstration of a complete power system would be the final phase.

REFERENCES

1. Kirk, J. A., P. A. Studer, and H. E. Evans, *Mechanical Capacitor*, NASA/GSFC TN D-8185, November 1975.

2. Michaels, T. D., E. W. Schliebin, and R. D. Scott, *Design Definition of a Mechanical Capacitor*, Final Report, NASA/GSFC, May 1977.

3. Scott, R. D., *Mechanical Capacitor Energy Storage System*, RCA, Advanced Technology Laboratories, Final Report, NASA Contract NAS 5-23650, February 1978.

4. Kirk, J. A., *Mechanical Capacitor – The Best Rim*, University of Maryland, November 1977.

5. Kirk, James A., "Flywheel Energy Storage-I Basic Concepts," *Int. J. Mech. Sci.*, Vol **19**, January 1977, pp. 223-231.

6. Kirk, James A., "Flywheel Energy Storage – II Magnetically Suspended Super Flywheel," *Int. J. Mech. Sci.*, Vol **19**, January 1977, pp. 233-245.

7. Slifer, Luther W., Jr., *Initial Guidelines and Estimates for a Power System with Inertial (Flywheel) Energy Storage*, NASA/GSFC TM 82134, December 1980.

8. Rodriguez, G. E., P. A. Studer, and L. W. Slifer, *Inertial Storage Power System Baseline Definition*, NASA/GSFC TM (in preparation), May 1981.

9. Corbett, Robert E., "High Voltage Power Systems For Military Needs," *Proceedings 15th Intersociety Energy Conversion Engineering Conference*, Vol **1**, No. 809137, August 18-22, 1980, pp. 715-719.

10. Segrest, Joseph D., "Advanced Aircraft Electric Power System," *Proceedings 16th Intersociety Energy Conversion Engineering Conference*, Vol **1**, No. 819081, August 9-14, 1981, pp. 127-129.

11. Reeiquam, E. T., "Power System Design for an All Electric Airplane," *Journal of Energy*, Vol **6**, No. 1 AIAA, January-February 1982.

12. Harris, D. W., "The Modular Power Subsystem for the Multimission Modular Spacecraft," *Proceedings 13th IECEC*, Vol **1**, No. 789003, August 1978.

13. Kichak, R. A., "The Standard Power Regulator for the Multimission Modular Spacecraft," *Proceedings 14th IECEC*, Vol **11**, August 5-10, 1979, pp. 1350-1355.

14. Studer, P. A., and H. E. Evans, "In-Space Inertial Energy Storage Design," *Proceedings 16th IECEC*, Vol **1**, August 9-14, 1981, pp. 74-79.

15. Millner, A. R., "A Flywheel Energy Storage and Conversion System for Solar Voltaic Applications," *American Society of Mechanical Engineers*, 79-Sol-1, March 1979.

16. Millner, A. R., and T. Dinwoodie, *System Design, Test Results, and Economic Analysis of a Flywheel Energy Storage and Conversion System for Photovoltaic Applications*, Presented at the IEEE PV Specialist Conference, January 7-10, 1980.

17. Millner, A. R., and R. D. Hay, "Flywheel Energy Storage Interface Unit for Photovoltaic Applications," *Proceedings 14th IECEC*, Vol 1, August 5-10, 1979, pp. 389-394.

18. Jarvinen, P. D., B. L. Brench, R. D. Hay, and N. E. Rassmusen, "Testing and Evaluation of a Solar Photovoltaic Flywheel Energy Storage System," *Proceedings 16th IECEC*, August 9-14, 1981, pp. 898-903.

19. Eisenhauer, D., J. Downer, and R. Hockney, *Factors Affecting the Control of a Magnetically Suspended Flywheel*, The Charles Stark Draper Laboratory, Inc., Cambridge, Massachusetts.

20. Eisenhauer, D., G. Oberdeck, S. O'Dea, and W. Stanton, *Final Report on Research Toward Improved Flywheel Suspension and Energy Conversion Systems*, The Charles Stark Draper Laboratory, Cambridge, Massachusetts, 1977.

21. Eisenhauer, D., and E. Kingsbury, *Final Report on the Development of an Advanced Flywheel Bearing Performance Model*, The Charles Stark Draper Laboratory, Cambridge, Massachusetts, 1978.

22. Eisenhauer, D., G. Oberdeck, and J. Downer, "Development of a Low Loss Flywheel Magnetic Bearing," *Proceedings 14th IECEC*, Vol 1, 1979, pp. 357-362.

23. Albrecht, P. R., J. Walowit, and O. Pinkus, "Analytical and Experimental Investigation of Magnetic Support Systems – Part II – Experimental Investigation," *The American Society of Mechanical Engineers*, 81-LUB-32, October 1981.

24. Studer, P. A., *Magnetic Bearing*, U.S. Patent 3865442, February 1975.

25. Studer, P. A., *Electric Motive Machine Including Magnetic Bearing*, U.S. Patent 3,694,041, September 1972.

26. Anderson, W. W., and N. J. Groom, *The Annular Momentum Control Device (AMCD) and Potential Applications*, NASA/Langley Research Center, TND-7866, March 1975.

27. Studer, P. A., and M. G. Gasser, *A Bi-Directional Linear Motor/Generator with Integral Magnetic Bearings for Long Lifetime Stirling Cycle Refrigerators*, NASA/GSFC.

28. Steele, R. S., "Composite Flywheel Balance Experience," *Proceedings 16th IECEC*, No. 819413, August 9-14, 1981.

29. Studer, Philip A., "A New D.C. Torque Motor," *2nd International Workshop on Rare Earth Cobalt Magnets and Their Applications*, University of Dayton, Dayton, Ohio, June 1976.

30. Demerdash, N. A., and T. W. Nehl, "Dynamic Modeling of Brushless D.C. Motor-Power Conditioner Unit for Electromechanical Actuator Application," *IEEE Power Electronics Specialist Conference*, June 1979.

31. Demerdash, N. A., and T. W. Nehl, *Closed Loop Performance of a Brushless D.C. Motor Powered by an Electromechanical Actuator for Flight Control Applications*, NAECON, May 1980.

32. Demerdash, N. A., and B. P. Overton, "Practical Application of Power Conditioning to Electric Propulsion for Passenger Vehicles," *IEEE Power Electronics Specialist Conference*, June 1980.

33. Demerdash, N. A., T. W. Nehl, and E. Maslowski, *Dynamic Modeling of Brushless D.C. Motors in Electric Propulsion and Electromechanical Actuation by Digital Techniques*, IAS Conference Record, September 1980.

34. Demerdash, N. A., and T. W. Nehl, "Dynamic Modeling of Brushless D.C. Motors for Aerospace Actuation," *IEEE Transactions on Aerospace and Electronic Systems*, Vol **AES-16**, November 1980.

35. Demerdash, N. A., R. H. Miller, T. W. Nehl, B. P. Overton, and C. J. Ford, "Comparison Between Features and Performance Characteristics of Fifteen HP Samarium Cobalt and Ferrite Based Brushless DC Motors Operated by Same Power Conditioner," *IEEE PES Winter Meeting*, New York, New York, February 1982.

36. Coppa, A. P., *Energy Storage Flywheel Housing Design Concept Development*, Subcontract No. 6624409 for Lawrence Livermore National Laboratory, Livermore, California.

37. Fisher, R. L., and P. A. Studer, "The Impact of Rare Earth Cobalt Permanent Magnets on Electromechanical Device Design," *13th Aerospace Mechanisms Symposium*, 1979.

38. Studer, Philip A., *Development of a Sealed Brushless DC Motor*, NASA/GSFC TN D-2819, May 1965.

39. Van Ommering, G., C. W. Koehler, and D. C. Briggs, "Nickel-Hydrogen Batteries for Intelsat V," *Proceedings 15th IECEC*, Vol 1, No. 809382, August 18-22, 1980, pp. 1885-1890.

40. Mueller, V. C., "Nickel-Hydrogen Battery Integration Study for the Multimission Modular Spacecraft," *Proceedings 15th IECEC*, Vol 1, No. 809385, August 18-22, 1980, pp. 1901-1907.

41. Notti, J. E., A. Cormack III, and W. C. Schmill, *Integrated Power/Attitude Control System (PACS) Study*, Vols I & II, NASA Contract Report, NASA CR-3383, April 1974.

42. Guyen, N., H. Nahia, and Marian Francois, *Study of System Implications of High Speed Flywheels as Energy Storage Devices on Satellites*, MATRA Note No. 30/1020, ESA Contract No. 3261/77/NL/AK, October 1978.

SOURCES

Annual Contractors' Review Meeting for DOE Physical and Chemical Storage Projects, Washington, D.C., August 23-26, 1982.

Cormack, A., III, and J. E. Notti, Jr., *Design Report for the Rotating Assembly for an Integrated Power/Attitude Control System*, Rockwell International, Space Division, NASA Contract NAS 1-13008, September 1974.

Davis, A., and A. Csomer, "The New Age of High Performance Kinetic Energy Storage Systems," *Proceedings 15th IECEC*, August 18-22, 1980, pp. 1507-1512.

Decker, D. K., J. Cassinelli, and M. Valgora, *High Power Solar Array Switching Regulation.*

Ginsburg, B. R., *RPE-10 Composite Flywheel Testing*, Rocketdyne Division, Rockwell International, Contract PO 9519409, Lawrence Livermore National Laboratory, June 15, 1981.

Green, A. K., *Guidelines for Selection of Fibre Reinforced Composite Materials for Spacecraft Applications*, R 878/1A, ESA Contract 4389/80/NL/AK/(SC), January 1982.

Hay, R. D., A. R. Millner, and P. O. Jarvin, "Residential Photovoltaic Flywheel Storage System Performance and Cost," *Proceedings 15th IECEC*, August 18-22, 1980, pp. 1528-1533.

Henry, E. A., *Research Leading to the Production and Early Use of Numeric Data Banks of Material Properties and System Analyses*, Lawrence Livermore Laboratory.

Kulkarni, Satish V., "Composite Material Flywheels and Containment Systems," *Energy and Technology Review*, Lawrence Livermore National Laboratory, March 1982, pp. 18-29.

Lanier, J. R., J. R. Graves, R. E. Kapustka, and J. R. Bush, Jr., "A Programmable Power Processor for High Power Space Applications," *IEEE Power Electronic Specialist Conference*, June 14-17, 1982.

Lukens, F. E., and R. L. Moser, *Programmable Power Processor (P^3)*.

McMurphy, Frederick E., and Terrence M. Quick, *Bibliographic and Numeric Data Bases for Fibre Composites and Matrix Materials*, Lawrence Livermore Laboratory, University of California, DOE Contract Number W-7405-ENG-48.

Rabenhorst, D. W., and W. O. Wilkinson, *Prototype Flywheel Spin Testing Program*, Final Report, The Johns Hopkins University, Applied Physics Laboratory, UCRL-15381, Subcontract No. 7825509, LLL, April 1981.

Robinson, A. A., *Magnetic Bearings — The Ultimate Means of Support for Moving Parts in Space*, Spacecraft Technology Department, ESA Technical Directorate, ESTEC, Noordwijk, Netherlands, Bulletin **26**.

Satchwell, David L., "High Energy Density Flywheel," *Proceedings 14th IECEC*, August 5-10, 1979.

Sheje, John R., Robert E. Corbett, and Michael C. Glass, *Series vs. Shunt Regulators for Power Control in Satellite Power Systems*.

Sollo, Charles, "Distribution Voltage for High-Power Satellites," *Proceedings 17th IECEC*, Vol 1, August 8-12, 1982, pp. 181-186.

U.S. Energy Research and Development Administration, *Proceedings of the 1975 Flywheel Technology Symposium*, Lawrence Hall of Science, Lawrence Livermore Laboratory, Berkeley, California, November 10-12, 1975.

U.S. Department of Energy, *1977 Flywheel Technology Symposium Proceedings*, Lawrence Livermore Laboratory, San Francisco, California, October 5-7, 1977.

U.S. Department of Energy, *1980 Flywheel Technology Symposium*, American Society of Mechanical Engineers, Lawrence Livermore National Laboratory, Scottsdale, Arizona, October 1980.